Optimization of Spatiotemporal Apertures in Channel Sounding

Pedersen, Troels; Pedersen, Claus; Yin, Xuefeng; Fleury, Bernard Henri

Published in:
IEEE Transactions on Signal Processing

DOI (link to publication from Publisher):
10.1109/TSP.2008.928967

Publication date:
2008

Document Version
Publisher's PDF, also known as Version of record

Optimization of Spatiotemporal Apertures in Channel Sounding

Troels Pedersen, *Student Member, IEEE*, Claus Pedersen, Xuefeng Yin, *Member, IEEE*, and Bernard H. Fleury, *Senior Member, IEEE*

***Abstract*—In this paper, we investigate the impact of the spatiotemporal aperture of a channel sounding system equipped with antenna arrays at the transmitter and receiver on the accuracy of joint estimation of Doppler frequency and bidirection. The contribution of this paper is threefold. First, we state a spatiotemporal model that can describe parallel as well as switched sounding systems. The proposed model is applicable for arbitrary layouts of the spatial arrays. To simplify the derivations, we investigate the special case of linear spatial arrays. However, the results obtained for linear arrays can be generalized to arbitrary arrays. Secondly, we give the necessary and sufficient conditions for a spatiotemporal array to yield the minimum Cramér–Rao lower bound (CRLB) in the single-path case and Bayesian CRLB in the multipath case. The obtained conditions amount to an orthogonality condition on the spatiotemporal array. Thirdly, we define the Doppler-bidirection ambiguity function and derive the necessary and sufficient conditions for a linear spatiotemporal array to be ambiguous. Based on the ambiguity function, we define the normalized side-lobe level, which we propose to use as a figure of merit in the design of spatiotemporal arrays.**

***Index Terms*—Ambiguity function, array processing, Cramér-Rao lower bound, high-resolution channel-parameter estimation, MIMO channel sounding, space–time sampling.**

I. Introduction

THE design and optimization of multiple-input multiple-output (MIMO) communication systems require realistic models of the propagation channel, which incorporate dispersion in delay, Doppler frequency, direction of departure, direction of arrival, and polarization. In order to develop realistic parametric models of the channel response, it is of great importance to be able to accurately measure the dispersive behavior of the propagation channel, that is, simultaneously measure dispersion in the above dimensions. Dispersion of the propagation channel in one dimension can be estimated from an observation using an aperture in the corresponding Fourier domain. For example, if Doppler frequency is to be estimated, observations at different time instants are required.

The focus of this paper is on the joint estimation of direction of departure, direction of arrival, and Doppler frequency from observations obtained by exciting the propagation channel via a *spatial aperture* and sensing the output of the channel via another spatial aperture at different time instants, i.e., via a *temporal aperture*. Altogether, these three apertures constitute a bispatiotemporal aperture, or a *spatiotemporal aperture* for short. A spatiotemporal aperture can be implemented using antenna arrays at the transmitter and receiver sites. Spatiotemporal sounding systems fall in two groups: parallel and switched sounding systems.

A *parallel* sounding system (such as [1]) is equipped with one transmitter for each transmit antenna element and one receiver per receive antenna element. All transmit array elements are active simultaneously and all outputs of the receive array elements are observed simultaneously. Snapshots of the channel are collected at different time instances. Each of the parallel transmitters must transmit a unique signal. The transmitted sounding signals must be carefully chosen such that their cross- and autocorrelation properties allow for their separation and sufficient delay resolution, respectively. In *switched* sounding systems (such as the one used in [2]–[5]), the sounding signal generated by a single transmitter is applied to the elements of the transmit array via a switch. The output of the receive array is sensed via another switch. In this way, observations from all antenna pairs of one transmit antenna and one receive antenna can be obtained. Despite the added switches, the hardware complexity of switched systems is lower than that of parallel systems. Furthermore, the cross-correlation properties of the sounding signals is not an issue in switched channel sounding systems, and therefore any code sequence with the desired autocorrelation property may be applied.

Various algorithms for the estimation of directions and Doppler shifts from data obtained from spatiotemporal arrays have been proposed; see, e.g., [2]–[5] and references therein. It is shown in [5] that the design of spatiotemporal apertures is critical to the joint estimation of Doppler frequency and bidirection. Until recently, it was believed that the maximum absolute Doppler frequency that can be estimated with a switched sounding system is inversely proportional to the product of the number of elements of the transmit and receive arrays.

Manuscript received July 6, 2007; revised May 26, 2008. First published July 25, 2008; current version published September 17, 2008. The associate editor coordinating the review of this manuscript and approving it for publication was Dr. Mats Bengtsson. This work was supported in part by Elektrobit, the European Commission within the FP7-ICT STREP project Wireless Hybrid Enhanced Mobile Radio Estimators, WHERE, under Contract 217033, and the FP7-ICT Network of Excellence in Wireless Communications, NEWCOM++, under Contract 216715..

T. Pedersen and X. Yin are with the Section of Navigation and Communications, Department of Electronic Systems, Aalborg University, DK-9220 Aalborg, Denmark (e-mail: troels@es.aau.dk; xuefeng@es.aau.dk).

B. H. Fleury is with the Section of Navigation and Communications, Department of Electronic Systems, Aalborg University, DK-9220 Aalborg, Denmark, and the Telecommunications Research Center Vienna, ftw., A-1220 Wien, Austria (e-mail: fleury@es.aau.dk).

C. Pedersen is with Vesteraa 28E, DK-9000 Aalborg, Denmark (e-mail: cped00@gmail.com).

Digital Object Identifier 10.1109/TSP.2008.928967

This limitation was considered a major drawback of switched systems [1]. However, as shown in [4] and [5], this limitation is the result of the (inappropriate) choice of the spatiotemporal aperture and is not a fundamental (Nyquist) limit. This inappropriate choice leads to an ambiguity in the estimation of Doppler frequency and direction [5]. An intuitive interpretation of this effect is that the phase changes induced by a plane wave at the outputs of the array elements may result either due to the fact that the wave exhibits a Doppler frequency or due to the wave's impinging direction, when a switched sounding system is used. The ambiguity effect occurs when it is not possible to distinguish which effect has really caused this phase change. In particular, it was shown in [5] that by appropriately selecting the spatiotemporal aperture, it is possible to extend the above maximum Doppler frequency to the largest value that can be estimated with a similar single-input single-output sounding system. As illustrated by these results, the theoretical understanding of the impact of the spatiotemporal aperture on joint bidirection and Doppler estimators requires a joint treatment of the spatiotemporal aperture.

In this paper, we investigate the impact of the spatiotemporal aperture on the accuracy of joint estimation of Doppler frequency and bidirection. The contribution of this work is threefold. First, we state a spatiotemporal model that can describe parallel as well as switched sounding systems. The proposed model is applicable for arbitrary layouts of the spatial arrays. However, to simplify the derivations, we investigate the special case of linear spatial arrays. Secondly, we give the necessary and sufficient conditions for a spatiotemporal array to yield the minimum Cramér-Rao lower bound (CRLB) in the single-path case and Bayesian CRLB (BCRLB) in the multipath case. The obtained conditions amount to an orthogonality condition on the spatiotemporal array. A similar condition for azimuth and elevation estimation has been derived in the single-path case for planar arrays in [6] and three-dimensional arrays in [7]. Thirdly, we define the Doppler-bidirection ambiguity function for the proposed spatiotemporal model. The ambiguity function [8] is a standard means to assess the resolution ability of radar waveforms and a rich literature exists on ambiguity functions and related results for various radar systems; see, e.g., [9] and [10] and references therein. In [11], the ambiguity function has been defined for MIMO bistatic radar systems with parallel transmitters and receivers. The interested reader is referred to this contribution for an overview and discussion of recent results on ambiguity functions for mono- and bistatic radar. The bistatic radar estimation problem is essentially the same as the problem of parameter estimation of single-bounce propagation paths in the field of channel sounding for MIMO wireless communications. However, in real propagation environments, single-bounce-only propagation cannot be assumed, and consequently the available radar results do not apply directly. In the channel sounding literature, however, the use of ambiguity functions has been fairly limited so far. In [12] and [13], the delay-Doppler ambiguity function is computed. To our best knowledge, the ambiguity function has not previously been defined and calculated for (bi)spatiotemporal channel sounding. The ambiguity function presented in this paper is valid for both parallel and switched sounding systems. It is a special case of the general ambiguity function defined in [9]. Based on this ambiguity function, we derive the necessary and sufficient conditions for a linear spatiotemporal array to be ambiguous. The obtained result generalizes the result from [5] and resembles the results of the well-studied type-1 (or rank-1) ambiguity effect for spatial arrays; see, e.g., [14]–[16]. Based on the ambiguity function, we also define the normalized side-lobe level (NSL), which we propose to use as a figure of merit in the design of spatiotemporal arrays.

This paper is organized as follows. In Section II, we introduce a model of the spatiotemporal sounding system capable of describing both parallel and switched systems. In Section III, the impact of the spatiotemporal array on the CRLB and the BCRLB is investigated. In Section IV, we define the Doppler-bidirection ambiguity function, which is then used for the analysis of the above-mentioned ambiguity effect. In Section V, we investigate the effect of the spatiotemporal aperture on the estimation performance by means of Monte Carlo simulations. Concluding remarks are stated in Section VI.

Notation: Throughout this contribution, the following notation is used. Vectors and matrices have boldfaced symbols. Sets are printed in calligraphic letters (such as $\mathcal{A}$). The notations $[\cdot]^*$, $[\cdot]^{\mathsf{T}}$, and $[\cdot]^{\mathsf{H}}$ denote complex conjugation, transposition, and Hermitian transposition, respectively. The notations $[\mathbf{a}]_p$ and $[\mathbf{A}]_{p,q}$ mean the pth element of the vector $\mathbf{a}$ and element (p,q) of the matrix $\mathbf{A}$. The symbol $\otimes$ denotes the Kronecker product. The notation $\mathbf{A} \succeq \mathbf{B}$ means that the matrix $\mathbf{A}-\mathbf{B}$ is positive semidefinite. We denote a p-dimensional column vector with unity entries by $\mathbf{1}_p$. The notation $|\cdot|$ stands for the Euclidean norm of a scalar or vector and the cardinal number of a set. Expectation is denoted by $\mathsf{E}[\cdot]$. The least integer larger than or equal to a is denoted by $\lceil a \rceil$. The symbols $\mathbb{Z}$, $\mathbb{R}$, and $\mathbb{C}$ stand for the set of integers, the real line, and the complex plane, respectively.

II. System Model

Let us consider the propagation environment depicted in Fig. 1. The sounding system consists of two antenna arrays referred to as Array 1 and Array 2, respectively. The index $k \in \{1,2\}$ is used to distinguish the transmitter $(k=1)$ from the receiver $(k=2)$. The number of elements in Array k is denoted by M_k. At Array k, the coordinates are given in carrier wavelengths with respect to the coordinate system O_k. The displacement of Array k element m_k from the origin of the coordinate system O_k is denoted by $\mathbf{r}_{k,m_k} \in \mathbb{R}^3$. To simplify the notation, we write $\mathbf{r}_{m_k}$ for $\mathbf{r}_{k,m_k}$. The time variable is denoted by $t \in \mathbb{R}$.

Referring to Fig. 1, a certain number L of waves propagate along different paths from Array 1 to Array 2. Along its path a wave interacts with a certain number of scatterers. We make the following assumptions on the propagation environment.

A) Following [2], we assume that the far-field condition holds, such that a plane wave approximation can be

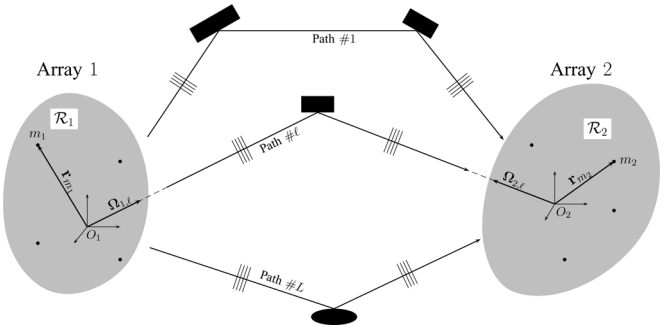

Fig. 1. The considered multipath propagation environment. The black dots in the regions $\mathcal{R}_1$ and $\mathcal{R}_2$ indicate the positions of the array elements.

applied in a region $\mathcal{R}_k \subset \mathbb{R}^3$ surrounding Array k when the other array transmits. This implies that the set of parameters describing each path is independent of the array element positions.

B) The propagation paths are assumed to be specular.

C) We assume that the geometry of the propagation paths is constant throughout the observation window $\mathcal{T}$. In other words, the parameters of the propagation paths remain constant for the whole measurement run.

D) We consider the narrow-band case only. Hence, without loss of generality propagation delays are assumed to be zero.

E) We assume that the elements of Array 1 and Array 2 are isotropic.

Under Assumptions A)–D), the ℓth path can be described by the parameter vector $\boldsymbol{\theta}_\ell \triangleq \left[\nu_\ell, \boldsymbol{\Omega}_{1,\ell}^{\mathsf{T}}, \boldsymbol{\Omega}_{2,\ell}^{\mathsf{T}}, \alpha_\ell\right]^{\mathsf{T}}$, where ν_ℓ is the Doppler frequency of Path ℓ and $\boldsymbol{\Omega}_{k,\ell}$ is a unit vector with the initial point anchored at the origin of O_k pointing towards the direction of Path ℓ in $\mathcal{R}_k$ (see Fig. 1). We denote the complex gain of path ℓ as α_ℓ. The $8L$-dimensional vector $\boldsymbol{\theta} \triangleq \left[\boldsymbol{\theta}_1^{\mathsf{T}}, \ldots, \boldsymbol{\theta}_L^{\mathsf{T}}\right]^{\mathsf{T}}$ contains the parameters of all L paths.

A. Signal Model

Let $p_{m_1}(t)$ be the (complex baseband representations of the) sounding signal applied to the input of Array 1 element m_1. We consider J nonoverlapping sounding intervals of length T. The center time instant of the jth sounding interval is denoted by t_j. Thus the jth sounding interval reads $\mathcal{T}_j = [t_j - (T/2), t_j + (T/2))$. The center time instants $t_1, \ldots t_J$ are selected such that $\mathcal{T}_1, \ldots, \mathcal{T}_J$ are disjoint. For both parallel and switched systems, the observation window $\mathcal{T} = \bigcup_{j=1}^{J} \mathcal{T}_j$ equals the union of the sounding intervals. Element m_1 of Array 1 is said to be *active* during $\mathcal{T}_j$ if $\mathcal{T}_j$ is a subset of the support of the signal $p_{m_1}(t)$, i.e., if the sounding waveform is fed to its input terminal. Similarly, an element of Array 2 is active during $\mathcal{T}_j$ if its output terminal is sensed during $\mathcal{T}_j$. Furthermore, we say that the antenna pair (m_1, m_2) is active during $\mathcal{T}_j$ if Array 1 element m_1 and Array 2 element m_2 are both active during $\mathcal{T}_j$.

For the sake of clarity, we first introduce the notation for a parallel sounding system. Thereafter, we consider switched sounding and describe a common model for both switched and parallel systems. Let $p_{j,m_1}(t)$ be the sounding pulse with support $\mathcal{T}_j$ applied to the input of Array 1 element m_1 of a parallel sounding system. Then $p_{m_1}(t)$ is of the form

$$p_{m_1}(t) = \sum_{j=1}^{J} p_{j,m_1}(t). \tag{1}$$

We consider the case where the sounding pulses have same energy E and are mutually orthogonal, i.e.,

$$\int_{\mathcal{T}} p_{j,m_1}(t) p^*_{j',m_1'}(t) \mathrm{d}t = E \cdot \delta_{jj'} \cdot \delta_{m_1 m_1'} \tag{2}$$

where $\delta..$ is the Kronecker delta function. This orthogonality restriction ensures that the signal contributions of different transmitted sounding pulses can be extracted from the received signal without interference from the other pulses. Furthermore, it implies that the noise contributions in the extracted sounding pulses are uncorrelated for different sounding pulses. In practice, the sounding pulses must be chosen to fulfill (2), at least approximately, e.g., by letting the sounding pulses at different transmitters be differently shifted versions of the same pseudonoise sequence.

The output signal of Array 2 element m_2 is given as

$$Y_{m_2}(t) = \sum_{m_1=1}^{M_1} \sum_{j=1}^{J} s_{j,m_1,m_2}(t, \boldsymbol{\theta}) + N_{m_2}(t), \quad t \in \mathcal{T} \tag{3}$$

where $s_{j,m_1,m_2}(t;\boldsymbol{\theta})$ and $N_{m_2}(t)$ denote, respectively, the *signal contribution* due to the jth sounding pulse applied to the input of Array 1 element m_1 and the *noise contribution* to $Y_{m_2}(t)$. The noise contributions across the Array 2 element outputs are assumed to be spatially and temporally white circularly symmetric complex Gaussian processes, i.e., fulfilling

$$\mathsf{E}\left[N_{m_2}(t) N_{m_2'}(t+\tau)^*\right] = N_0 \cdot \delta_{m_2,m_2'} \cdot \delta(\tau) \tag{4}$$

where N_0 is a positive constant and $\delta(\cdot)$ denotes the Dirac delta function.

Under the Assumptions A)–E), we can write the signal contribution $s_{j,m_1,m_2}(t;\boldsymbol{\theta})$ as

$$s_{j,m_1,m_2}(t;\boldsymbol{\theta}) = \sum_{\ell=1}^{L} \alpha_\ell \exp\left(j2\pi\left(\nu_\ell t + \boldsymbol{\Omega}_{1,\ell}^{\mathsf{T}} \mathbf{r}_{m_1} + \boldsymbol{\Omega}_{2,\ell}^{\mathsf{T}} \mathbf{r}_{m_2}\right)\right) p_{j,m_1}(t). \tag{5}$$

B. Maximum-Likelihood Estimation of Path Parameters

First we introduce a notation that clearly distinguishes among the parameter of the propagation paths, their estimates, and the free parameter in the log-likelihood function. We adhere to the following notational convention: $\hat{(\cdot)}$ is an estimate of the parameter given as argument and $\bar{(\cdot)}$ is a free parameter in the log-likelihood function. As an example, the symbol ν_ℓ denotes the Doppler frequency of Path ℓ, of which the estimate $\hat{\nu}_\ell$ is obtained by joint maximization of the log-likelihood function $\Lambda(\bar{\boldsymbol{\theta}})$ with respect to $\bar{\nu}_\ell$ and the remaining free parameters of $\bar{\boldsymbol{\theta}}$.

In the sequel, we consider the maximum-likelihood estimator of the parameter vector $\boldsymbol{\theta}$

$$\widehat{\boldsymbol{\theta}} = \arg\max_{\bar{\boldsymbol{\theta}} \in \mathcal{E}_{\boldsymbol{\theta}}} \Lambda(\bar{\boldsymbol{\theta}}) \tag{6}$$

where $\Lambda(\bar{\boldsymbol{\theta}})$ is the log-likelihood of $\bar{\boldsymbol{\theta}}$ given an observation $y_1(t), \ldots, y_{M_2}(t)$ of the processes $Y_1(t), \ldots, Y_{M_2}(t)$ and $\mathcal{E}_{\cdot}$ denotes the estimation range of the parameter given as index. The maximization in (6) is over the $8L$-dimensional domain $\mathcal{E}_{\boldsymbol{\theta}}$.[1]

The log-likelihood of $\bar{\boldsymbol{\theta}}$ given an observation $y_1(t), \ldots, y_{M_2}(t)$ of $Y_1(t), \ldots, Y_{M_2}(t)$ reads [2], [17]

$$\Lambda(\bar{\boldsymbol{\theta}}) = \sum_{m_2=1}^{M_2} \left\{ 2\Re \left[\int_{\mathcal{T}} \sum_{j=1}^{J} y_{m_2}(t) \sum_{m_1=1}^{M_1} s^*_{j,m_1,m_2}(t;\bar{\boldsymbol{\theta}}) \mathrm{d}t \right] - \int_{\mathcal{T}} \left| \sum_{j=1}^{J} \sum_{m_1=1}^{M_1} s_{j,m_1,m_2}(t;\bar{\boldsymbol{\theta}}) \right|^2 \mathrm{d}t \right\}. \tag{7}$$

Due to the orthogonality (2) of the transmitted pulses, all "cross terms" in the leftmost integral of (7) vanish. Thus, (7) simplifies to the triple sum

$$\Lambda(\bar{\boldsymbol{\theta}}) = \sum_{j=1}^{J} \sum_{m_1=1}^{M_1} \sum_{m_2=1}^{M_2} \Lambda_{j,m_1,m_2}(\bar{\boldsymbol{\theta}}) \tag{8}$$

where the summands are defined as

$$\Lambda_{j,m_1,m_2}(\bar{\boldsymbol{\theta}}) \triangleq 2\Re\left\{ H_{j,m_1,m_2}(\bar{\boldsymbol{\theta}}) \right\} - E_{j,m_1,m_2}(\bar{\boldsymbol{\theta}}) \tag{9}$$

with

$$H_{j,m_1,m_2}(\bar{\boldsymbol{\theta}}) \triangleq \int_{\mathcal{T}_j} y_{m_2}(t) s^*_{j,m_1,m_2}(t;\bar{\boldsymbol{\theta}}) \mathrm{d}t \tag{10}$$

and

$$E_{j,m_1,m_2}(\bar{\boldsymbol{\theta}}) \triangleq \int_{\mathcal{T}_j} \left| s_{j,m_1,m_2}(t;\bar{\boldsymbol{\theta}}) \right|^2 \mathrm{d}t. \tag{11}$$

The integral $H_{j,m_1,m_2}(\bar{\boldsymbol{\theta}})$ can be split into a signal term and a noise term. Inserting (3) and dropping the terms that are zero due to the orthogonality condition given in (2), we obtain

$$H_{j,m_1,m_2}(\bar{\boldsymbol{\theta}}) = \int_{\mathcal{T}_j} s_{j,m_1,m_2}(t,\boldsymbol{\theta}) s^*_{j,m_1,m_2}(t,\bar{\boldsymbol{\theta}}) \mathrm{d}t + \underbrace{\int_{\mathcal{T}_j} N_{m_2}(t) s^*_{j,m_1,m_2}(t,\bar{\boldsymbol{\theta}}) \mathrm{d}t}_{\triangleq N_{j,m_1,m_2}(\bar{\boldsymbol{\theta}})}. \tag{12}$$

Remembering that the noise contributions are temporally and spatially white, and applying the orthogonality assumption (2), the complex Gaussian random variables $N_{j,m_1,m_2}(\bar{\boldsymbol{\theta}})$ are uncorrelated

$$\mathsf{E}\left[N_{j,m_1,m_2}(\bar{\boldsymbol{\theta}}) N^*_{j',m'_1,m'_2}(\bar{\boldsymbol{\theta}}) \right] = E_{j,m_1,m_2}(\bar{\boldsymbol{\theta}}) \cdot N_0 \cdot \delta_{j,j'} \cdot \delta_{m_1,m'_1} \cdot \delta_{m_2,m'_2}. \tag{13}$$

C. Sounding Modes and Their Spatiotemporal Aperture Matrices

In the following, we generalize the system model such that it can account for any configuration of switched and parallel transmitters and receivers. Motivated by the particular form of (8), we use the term *spatiotemporal sample* to denote the signal component that was transmitted from Array 1 element m_1, received at Array 2 element m_2 during $\mathcal{T}_j$. Each sample results in one term of the sum in (8). Therefore, each spatiotemporal sample can be indexed by the triplet (j, m_1, m_2). In (8), the spatiotemporal samples are obtained from all combinations of one Array 1 element and one Array 2 element for every sounding interval. It follows readily from the derivation of (8) that if any of the spatiotemporal samples are left out, the corresponding terms in (8) will disappear. For instance, in a switched system, $\Lambda(\bar{\boldsymbol{\theta}})$ have a similar form, but the triple sum in (8) will only be over a subset of the set of all triplets (j, m_1, m_2).

Definition 1 (Sounding Mode): A sounding mode is a subset $\mathcal{M}$ of $\{1, \ldots, J\} \times \{1, \ldots, M_1\} \times \{1, \ldots, M_2\}$.

The log-likelihood function of $\bar{\boldsymbol{\theta}}$ associated to the sounding mode $\mathcal{M}$ is given by

$$\Lambda(\bar{\boldsymbol{\theta}}) = \sum_{(j,m_1,m_2) \in \mathcal{M}} \Lambda_{j,m_1,m_2}(\bar{\boldsymbol{\theta}}). \tag{14}$$

We enumerate the elements of a sounding mode $\mathcal{M}$ by the index i, i.e., we define a bijection

$$\{1, \ldots, I\} \to \mathcal{M}, \quad i \mapsto (j(i), m_1(i), m_2(i)). \tag{15}$$

Thus, $j(i)$ specifies in which sounding interval sample i was generated. Similarly, the indexes $m_1(i)$ and $m_2(i)$ specify which element of Array 1 and which element of Array 2, respectively, is used to generate sample i. The total number of spatiotemporal samples acquired in a measurement run is $I = |\mathcal{M}|$. Thus for a parallel sounding system, where $\mathcal{M} = \{1, \ldots, J\} \times \{1, \ldots, M_1\} \times \{1, \ldots, M_2\}$, the number of samples is $I = JM_1M_2$. For a switched sounding system where one sample is acquired in each sounding interval, we have $I = J$.

Defining $\Lambda_i(\bar{\boldsymbol{\theta}}) \triangleq \Lambda_{(j(i),m_1(i),m_2(i))}(\bar{\boldsymbol{\theta}})$, we can now recast (14) as

$$\Lambda(\bar{\boldsymbol{\theta}}) = \sum_{i=1}^{I} \Lambda_i(\bar{\boldsymbol{\theta}}). \tag{16}$$

The choice of indexing in (15) is not unique. The particular enumeration of the elements of a sounding mode only determines the order of the terms in the sum (16), which is irrelevant in the further development. The indexing can therefore be selected

[1]The maximization over $\mathcal{E}_{\boldsymbol{\theta}}$ is computationally prohibitive. However, a low-complexity approximation of the maximum likelihood estimate can be obtained using a space-alternating generalized expectation-maximization algorithm [2]–[5].

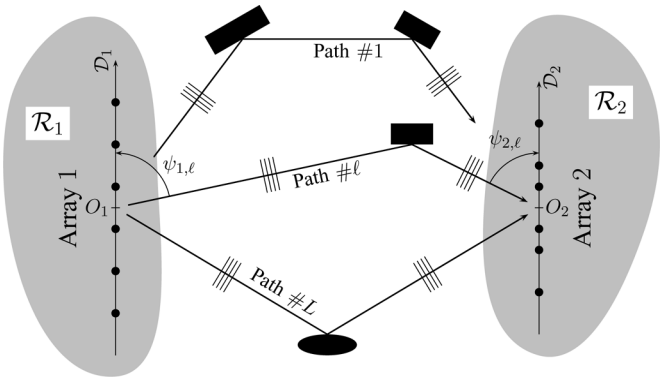

Fig. 2. A sounding system with linear arrays. The black dots indicate the centroids of the antenna elements.

arbitrarily by the system designer. In switched sounding systems, it is natural to select the indexes such that $j(i) = i$ and $t_1 < t_2 < \cdots < t_I$. In parallel sounding systems, however, indexing purely according to the temporal order is not possible because the sounding pulses overlap in time.

We define the vector

$$\mathbf{a}_i \triangleq \left[t(i), \mathbf{r}_1(i)^{\mathsf{T}}, \mathbf{r}_2(i)^{\mathsf{T}}\right]^{\mathsf{T}} \in \mathbb{R}^7 \tag{17}$$

where $t(i) \triangleq t_{j(i)}$, $\mathbf{r}_1(i) \triangleq \mathbf{r}_{m_1(i)}$, and $\mathbf{r}_2(i) \triangleq \mathbf{r}_{m_2(i)}$. We say that $\mathbf{a}_i$ is the center point of the ith spatiotemporal sample.

Definition 2 (Spatiotemporal Aperture Matrix): The $7 \times I$ spatiotemporal aperture matrix $\mathbf{A}$ is determined as

$$\mathbf{A} \triangleq [\mathbf{a}_1, \ldots, \mathbf{a}_i, \ldots, \mathbf{a}_I] \in \mathbb{R}^{7 \times I} \tag{18}$$

with $\mathbf{a}_i$ defined in (17).

Without loss of generality, we select the origin of the spatiotemporal coordinate system such that the columns of $\mathbf{A}$ fulfill

$$\sum_{i=1}^{I} \mathbf{a}_i = \mathbf{0}. \tag{19}$$

However, as we will see in Section III-A, this condition has some optimality property, in the sense that it ensures decoupling in the Fisher information matrix between the linear (α_ℓ) and nonlinear $(\boldsymbol{\vartheta}_\ell)$ parameters of path ℓ. The spatiotemporal aperture is uniquely defined by the spatiotemporal aperture matrix $\mathbf{A}$ together with the pulse length T.

D. Linear Antenna Arrays

For sounding systems with linear antenna arrays, as the one depicted in Fig. 2, the signal model can be simplified. We say that Array k is linear if its elements are located along a straight line $\mathcal{D}_k$ through the origin of O_k, i.e., $\mathbf{r}_k \in \mathcal{D}_k \cap \mathcal{R}_k$. In this case, the position of a point on the array axis $\mathcal{D}_k$ is specified by the signed distance $d_k \in \mathbb{R}$ from the origin of O_k. Likewise, $d_k(i)$ denotes the centroid position of the ith temporal sounding pulse at Array k. Obviously, the full $\boldsymbol{\Omega}_{k,\ell}$-vector cannot be estimated in this case but only its projection onto the array axis $\mathcal{D}_k$. Therefore, we replace $\boldsymbol{\Omega}_{k,\ell}$ by this projection, denoted by $\omega_{k,\ell}$. It can be noticed that $\omega_{k,\ell} = \cos(\psi_{k,\ell})$, where $\psi_{k,\ell}$ is the angle between the array axis $\mathcal{D}_k$ and $\boldsymbol{\Omega}_{k,\ell}$. We call $\omega_{k,\ell}$ the *spatial frequency* of Path ℓ at Array k. In the sequel, we assume one-dimensional arrays and replace $\mathbf{r}_k$ by d_k and $\boldsymbol{\Omega}_{k,\ell}$ by $\omega_{k,\ell}$. Consequently, $\mathbf{a}_i = [t(i), d_1(i), d_2(i)]^{\mathsf{T}} \in \mathbb{R}^3$, $\boldsymbol{\theta}_\ell = [\alpha_\ell, \nu_\ell, \omega_{1,\ell}, \omega_{2,\ell}]^{\mathsf{T}} \in \mathbb{C} \times \mathbb{R}^3$, and $\boldsymbol{\theta} = \left[\boldsymbol{\theta}_1^{\mathsf{T}}, \ldots, \boldsymbol{\theta}_L^{\mathsf{T}}\right]^{\mathsf{T}}$ is a $4L$-dimensional vector throughout the remainder of this paper. We also define $\boldsymbol{\vartheta}_\ell \triangleq [\nu_\ell, \omega_{1,\ell}, \omega_{2,\ell}]^{\mathsf{T}} \in \mathbb{R}^3$ and $\boldsymbol{\vartheta} \triangleq \left[\boldsymbol{\vartheta}_1^{\mathsf{T}}, \ldots, \boldsymbol{\vartheta}_L^{\mathsf{T}}\right]^{\mathsf{T}}$ for the subsequent investigations.

E. Specific Examples of Systems Using Linear Arrays

In numerical examples, we will consider two switched systems named "MIMO-ULA" and "SIMO-ULA." The MIMO-ULA system is equipped with two uniformly spaced linear arrays consisting of M_k antenna elements with half-wavelength interelement spacing. The position of element $m_k(i)$ is given by $d_k(i) \triangleq (m_k(i) - \mu_k)/2$, where μ_k is selected such that (19) is fulfilled. We define the antenna element index vector $\mathbf{m}_k \triangleq [m_k(1), \ldots, m_k(I)]^{\mathsf{T}}$. The SIMO-ULA system is a MIMO-ULA system with $M_1 = 1$. For both MIMO-ULA and SIMO-ULA, the uniform temporal sampling

$$t(i) \triangleq \left(i - \frac{I+1}{2}\right) T_r, \quad T_r \geq T \tag{20}$$

is selected. Here, T_r denotes the time period between consecutive samples. With this definition, $\sum_{i=1}^{I} t(i) = 0$, as required from (19). Hence, the spatiotemporal aperture matrix $\mathbf{A}$ of the MIMO-ULA system is fully defined by the vectors $\mathbf{m}_1$ and $\mathbf{m}_2$. For the SIMO-ULA system, it suffices to specify $\mathbf{m}_2$.

For the MIMO-ULA system, the estimation range $\mathcal{E}_{\boldsymbol{\vartheta}_\ell}$ of $\boldsymbol{\vartheta}_\ell$ is given as

$$\mathcal{E}_{\boldsymbol{\vartheta}_\ell} = \mathcal{E}_\nu \times \mathcal{E}_{\omega_1} \times \mathcal{E}_{\omega_2} \tag{21}$$

with $\mathcal{E}_\nu = (-1/(2T_r), +1/(2T_r)]$ and $\mathcal{E}_{\omega_k} = (-1, +1]$. For the SIMO-ULA system, where $\omega_{1,\ell}$ is not estimable, we select $\mathcal{E}_{\omega_1} = \{0\}$.

III. Fisher Information Matrix and Cramér–Rao Lower Bounds

In this section, we investigate the effect of the spatiotemporal aperture matrix $\mathbf{A}$ on the (conditional) CRLB and on the BCRLB for the estimation of the entries of the parameter vector $\boldsymbol{\theta}$. The CRLB is a function of $\boldsymbol{\theta}$, whereas the BCRLB depends on an assumed prior density function for $\boldsymbol{\theta}$ [18].

In Section III-A–E, we first derive the CRLB for the estimator and show which criterion the aperture matrix should fulfill in order to yield the minimum CRLB in a scenario with one propagation path $(L = 1)$. Thereafter, we show that the same criterion minimizes the BCRLB in the multipath case.

A. The Conditional Cramér–Rao Lower Bound

The CRLB on the variance of the estimation error of an unbiased estimator of $[\boldsymbol{\theta}]_{p,p}$ can be calculated as the pth diagonal element of the inverted Fisher information matrix

$$\mathrm{CRLB}([\hat{\boldsymbol{\theta}}]_p) \triangleq \left[\mathbf{F}(\boldsymbol{\theta})^{-1}\right]_{p,p}. \tag{22}$$

In Appendix I, the Fisher information matrix $\mathbf{F}(\boldsymbol{\theta})$ for the estimation of $\boldsymbol{\theta}$ is shown to be of the form

$$\mathbf{F}(\boldsymbol{\theta}) \triangleq \begin{bmatrix} \mathbf{F}_{\boldsymbol{\theta}_1\boldsymbol{\theta}_1} & \dots & \mathbf{F}_{\boldsymbol{\theta}_1\boldsymbol{\theta}_L} \\ \vdots & \ddots & \vdots \\ \mathbf{F}_{\boldsymbol{\theta}_L\boldsymbol{\theta}_1} & \dots & \mathbf{F}_{\boldsymbol{\theta}_L\boldsymbol{\theta}_L} \end{bmatrix} \tag{23}$$

where the submatrix $\mathbf{F}_{\boldsymbol{\theta}_\ell,\boldsymbol{\theta}_{\ell'}}$ is partitioned as

$$\mathbf{F}_{\boldsymbol{\theta}_\ell\boldsymbol{\theta}_{\ell'}} = \begin{bmatrix} F_{\alpha_\ell\alpha_{\ell'}} & \mathbf{F}_{\alpha_\ell\boldsymbol{\vartheta}_{\ell'}} \\ \mathbf{F}_{\boldsymbol{\vartheta}_\ell\alpha_{\ell'}} & \mathbf{F}_{\boldsymbol{\vartheta}_\ell\boldsymbol{\vartheta}_{\ell'}} \end{bmatrix}. \tag{24}$$

Defining the *normalized element factor* of sounding pulse i (see also Section IV) as

$$\mathrm{EF_n}(\nu;i) \triangleq \frac{1}{E}\int |p_i(t)|^2 \exp(j2\pi\nu t)\mathrm{d}t \tag{25}$$

with $p_i(t) \triangleq p_{j(i),m_1(i)}(t)$, the entries $\mathbf{F}_{\alpha_\ell\alpha_{\ell'}}, \mathbf{F}_{\boldsymbol{\vartheta}_\ell\alpha_{\ell'}} = \mathbf{F}^{\mathsf{H}}_{\alpha_{\ell'}\boldsymbol{\vartheta}_\ell}$, and $\mathbf{F}_{\boldsymbol{\vartheta}_\ell\boldsymbol{\vartheta}_{\ell'}}$ of $\mathbf{F}_{\boldsymbol{\theta}_\ell\boldsymbol{\theta}_{\ell'}}$ read

$$\mathbf{F}_{\alpha_\ell\alpha_{\ell'}} = \frac{E}{N_0}\Re\Bigg\{\sum_{i=1}^{I}\exp\left(j2\pi(\boldsymbol{\vartheta}_\ell-\boldsymbol{\vartheta}_{\ell'})^{\mathsf{T}}\mathbf{a}_i\right) \times \mathrm{EF_n}\left(\nu_\ell-\nu_{\ell'};i\right)\Bigg\} \tag{26}$$

$$\mathbf{F}_{\boldsymbol{\vartheta}_\ell\alpha_{\ell'}} = \frac{2\pi E}{N_0}\Re\Bigg\{(j-1)\alpha_{\ell'}\sum_{i=1}^{I}\mathbf{a}_i\cdot\exp\left(j2\pi(\boldsymbol{\vartheta}_\ell-\boldsymbol{\vartheta}_{\ell'})^{\mathsf{T}}\mathbf{a}_i\right) \times \mathrm{EF_n}\left(\nu_\ell-\nu_{\ell'};i\right)\Bigg\} \tag{27}$$

and

$$\mathbf{F}_{\boldsymbol{\vartheta}_\ell\boldsymbol{\vartheta}_{\ell'}} = \frac{8\pi^2 E}{N_0}\Re\Bigg\{\alpha_\ell\alpha^*_{\ell'}\sum_{i=I}^{I}\mathbf{a}_i\mathbf{a}_i{}^{\mathsf{T}}\exp(j2\pi(\boldsymbol{\vartheta}_\ell-\boldsymbol{\vartheta}_{\ell'})^{\mathsf{T}}\mathbf{a}_i) \times \mathrm{EF_n}(\nu_\ell-\nu_{\ell'};i)\Bigg\}. \tag{28}$$

As can be noticed from (26)–(28), the matrix $\mathbf{F}_{\boldsymbol{\theta}_\ell\boldsymbol{\theta}_{\ell'}}$ in general depends on the parameter vectors $\boldsymbol{\theta}_\ell$ and $\boldsymbol{\theta}_{\ell'}$. For $\ell = \ell'$, the factor $\mathrm{EF}_n(\nu;i)$ in (25) and the exponential terms in (26)–(28) are all unity. Therefore, making use of (19) and the identity $\sum_{i=1}^{I}\mathbf{a}_i\mathbf{a}_i{}^{\mathsf{T}} = \mathbf{A}\mathbf{A}^{\mathsf{T}}$, we obtain

$$\begin{aligned} \mathbf{F}_{\alpha_\ell\alpha_\ell} &= \frac{EI}{N_0}, \quad \mathbf{F}_{\boldsymbol{\vartheta}_\ell\alpha_\ell} = \mathbf{0}, \text{ and} \\ \mathbf{F}_{\boldsymbol{\vartheta}_\ell\boldsymbol{\vartheta}_\ell} &= \frac{8\pi^2 E|\alpha_\ell|^2}{N_0}\mathbf{A}\mathbf{A}^{\mathsf{T}}. \end{aligned} \tag{29}$$

As is apparent from (29), the matrix $\mathbf{F}_{\boldsymbol{\vartheta}_\ell\boldsymbol{\vartheta}_\ell}$ depends only on $|\alpha_\ell|$ and not on the remaining entries of $\boldsymbol{\theta}$. Notice that the choice of a coordinate system satisfying (19) ensures that $\mathbf{F}_{\boldsymbol{\vartheta}_\ell\alpha_\ell} = \mathbf{0}$ holds. Similar effects have previously been noticed for radar systems [19], for direction estimation [6] and for switched sounding systems [2].

B. The One-Path Case, Orthogonal Aperture

For the one-path case ($L = 1$), we have $\boldsymbol{\theta} = \boldsymbol{\theta}_1$. For simplicity, we drop the path index $\ell = 1$. It follows from (23), (24), and (29) that the Fisher information matrix reads

$$\mathbf{F}(\boldsymbol{\theta}) = \begin{bmatrix} \frac{EI}{N_0} & \mathbf{0}^{\mathsf{T}} \\ \mathbf{0} & \mathbf{F}_{\boldsymbol{\vartheta}\boldsymbol{\vartheta}} \end{bmatrix} \tag{30}$$

with

$$\begin{aligned} \mathbf{F}_{\boldsymbol{\vartheta}\boldsymbol{\vartheta}} &= 8\pi^2\gamma_{\mathrm{o}}\frac{1}{I}\mathbf{A}\mathbf{A}^{\mathsf{T}} \\ &= 8\pi^2\gamma_{\mathrm{o}}\frac{1}{I}\begin{bmatrix} \mathbf{t}^{\mathsf{T}}\mathbf{t} & \mathbf{t}^{\mathsf{T}}\mathbf{d}_1 & \mathbf{t}^{\mathsf{T}}\mathbf{d}_2 \\ \mathbf{d}_1^{\mathsf{T}}\mathbf{t} & \mathbf{d}_1^{\mathsf{T}}\mathbf{d}_1 & \mathbf{d}_1^{\mathsf{T}}\mathbf{d}_2 \\ \mathbf{d}_2^{\mathsf{T}}\mathbf{t} & \mathbf{d}_2^{\mathsf{T}}\mathbf{d}_1 & \mathbf{d}_2^{\mathsf{T}}\mathbf{d}_2 \end{bmatrix} \end{aligned} \tag{31}$$

where $\gamma_{\mathrm{o}} \triangleq |\alpha|^2(EI/N_0)$ is the signal-to-noise ratio (SNR) and $\mathbf{t} \triangleq [t(1),\dots,t(I)]^{\mathsf{T}}$, $\mathbf{d}_k \triangleq [d_k(1),\dots,d_k(I)]^{\mathsf{T}}$, $k = 1,2$, denote the rows of $\mathbf{A}$.

By inspection of (31), we see that the pth diagonal element of $\mathbf{F}_{\boldsymbol{\vartheta}\boldsymbol{\vartheta}}$ depends only on the squared norm of the pth row of $\mathbf{A}$, e.g., element (1,1) depends only on $|\mathbf{t}|^2$. The off-diagonal elements of $\mathbf{F}_{\boldsymbol{\vartheta}\boldsymbol{\vartheta}}$ are cross-terms involving scalar products of different rows of $\mathbf{A}$. For example, the off-diagonal element $[\mathbf{F}_{\boldsymbol{\vartheta}\boldsymbol{\vartheta}}]_{2,1}$ is proportional to $\mathbf{d}_1^{\mathsf{T}}\mathbf{t}$.

Theorem 3: The CRLBs for the estimation of the Doppler and spatial frequencies fulfill the inequalities

$$\begin{aligned} \mathrm{CRLB}(\hat{\omega}_k) &\geq \frac{1}{8\pi^2\gamma_{\mathrm{o}}\frac{1}{I}|\mathbf{d}_k|^2}, \quad k = 1,2 \\ \mathrm{CRLB}(\hat{\nu}) &\geq \frac{1}{8\pi^2\gamma_{\mathrm{o}}\frac{1}{I}|\mathbf{t}|^2}. \end{aligned} \tag{32}$$

Moreover, equality in all three inequalities is achieved simultaneously in (32) if and only if the rows of $\mathbf{A}$ are orthogonal, i.e.,

$$\mathbf{t}^{\mathsf{T}}\mathbf{d}_1 = 0, \quad \mathbf{t}^{\mathsf{T}}\mathbf{d}_2 = 0, \text{ and } \mathbf{d}_1^{\mathsf{T}}\mathbf{d}_2 = 0. \tag{33}$$

Proof: It is shown in [20, pp. 231] that $[\mathbf{F}]^{-1}_{p,p} \leq [\mathbf{F}^{-1}]_{p,p}$ for any p, i.e., $[\mathbf{F}]^{-1}_{p,p}$ lower bounds the CRLB for parameter $[\boldsymbol{\theta}]_p$. Using Lemma 19 given in Appendix II, we see that the equality $[\mathbf{F}_{\boldsymbol{\theta}\boldsymbol{\theta}}]^{-1}_{p,p} = \left[\mathbf{F}^{-1}_{\boldsymbol{\theta}\boldsymbol{\theta}}\right]_{p,p}$ is obtained for all p if and only if $\mathbf{F}_{\boldsymbol{\theta}\boldsymbol{\theta}}$ is diagonal. By inspection of (30), we see that $\mathbf{F}_{\boldsymbol{\theta}\boldsymbol{\theta}}$ is diagonal if and only if the rows of $\mathbf{A}$ fulfill (33). ■

Restricting the comparison to the class of apertures with equal diagonal elements in their associated Fisher information matrices, we have the corollary:

Corollary 4: Within the class of spatiotemporal apertures with identical values of $|\mathbf{t}|^2$, $|\mathbf{d}_1|^2$, and $|\mathbf{d}_2|^2$, the minimum CRLB is obtained if and only if the rows of the aperture matrix are orthogonal.

In the literature there exists a result for the joint estimation of elevation and azimuth of a single path analogous to Theorem 3. As shown in [6] and [7], the minimum CRLB for joint estimation of azimuth and elevation from data collected with a three-dimensional array is achieved if and only if the nondiagonal terms of the matrix $\sum_{i=1}^{I}\mathbf{r}_2(i)\mathbf{r}_2(i)^{\mathsf{T}}$ vanish.

C. Specific Examples (Continued)

In the following, we demonstrate the impact of the spatiotemporal aperture on the CRLB in the one-path case. We consider the CRLB of an MIMO-ULA system with $I = M_1 M_2$ and the commonly used sequential sounding mode

$$m_1(i) = \left\lceil \frac{i}{M_2} \right\rceil \tag{34}$$

$$m_2(i) = (i - 1 \bmod M_2) + 1. \tag{35}$$

Equivalently, $\mathbf{m}_1 = [1, 2, \ldots, M_1]^{\mathsf{T}} \otimes \mathbf{1}_{M_2}$ and $\mathbf{m}_2 = \mathbf{1}_{M_1} \otimes [1, 2, \ldots, M_2]^{\mathsf{T}}$. We chose $T_r = T$. This selection of $m_k(i)$ ensures that all pairs of one Array 1 element and one Array 2 element are active once, and, as we will show in Section III-E, that $\mathbf{d}_1^{\mathsf{T}} \mathbf{d}_2 = 0$. The resulting spatiotemporal aperture matrix yields a nondiagonal Fisher information matrix because $\mathbf{t}^{\mathsf{T}} \mathbf{d}_k \neq 0$ and the minimum CRLB is not obtained. If in addition $M_1 = M_2$, the Fisher information matrix is noninvertible, and hence the CRLB is infinite. For instance, in the case where $M_1 = 10$ and $M_2 = 9$, the ratios between the CRLBs obtained for the selected aperture matrix $\mathbf{A}$ resulting from (34) and (35) and the minimum CRLB for ν, ω_1, and ω_2 are calculated as $\left[\mathbf{F}_{\boldsymbol{\theta}\boldsymbol{\theta}}^{-1}\right]_{2,2} \cdot [\mathbf{F}_{\boldsymbol{\theta}\boldsymbol{\theta}}]_{2,2} \approx 15.4$ dB, $\left[\mathbf{F}_{\boldsymbol{\theta}\boldsymbol{\theta}}^{-1}\right]_{3,3} \cdot [\mathbf{F}_{\boldsymbol{\theta}\boldsymbol{\theta}}]_{3,3} \approx 15.3$ dB, and $\left[\mathbf{F}_{\boldsymbol{\theta}\boldsymbol{\theta}}^{-1}\right]_{4,4} \cdot [\mathbf{F}_{\boldsymbol{\theta}\boldsymbol{\theta}}]_{4,4} \approx 1.27$ dB, respectively.

In the above example, the spatial sounding was selected such that all antenna array elements are active the same number of times during one measurement run. In the next example, we compare this case to that where some antenna elements are active more frequently than others. With $M_k = 8, k = 1, 2$ we see that $|\mathbf{d}_k|^2 = 84$ if all Array k elements are active eight times. For comparison, we select the spatial sampling schemes such that $m_k(i) \in \{1, 2, 7, 8\}$, i.e., we use only four of the eight elements of each array. In this case, provided all the used antenna array elements are active the same number of times (i.e., 16 times) during the measurement run, we have $|\mathbf{d}_k|^2 = 148$. If both spatiotemporal apertures fulfill (33), we see that the CRLB in the latter case is lower than in the former case. The difference amounts to approximately 2.46 dB.

These two examples clearly show that the sounding mode highly affects the CRLBs for the estimation of spatial and Doppler frequencies in the one-path case.

D. Orthogonal Apertures in the Multipath Case

Motivated by the above orthogonality criterion that applies to the one-path case, it is of interest to see if this condition holds true in the multipath case as well. As remarked in Section III-A, the Fisher information matrix depends on the parameters to be estimated. In particular, the off-diagonals of the Fisher information matrix which enters the proof of Theorem 3 depend on the path parameters. Thus it is difficult to give a characterization of the minimum CRLB in the multipath case. To circumvent this obstacle, we investigate the BCRLB.

The BCRLB for the estimation of $\boldsymbol{\theta}$ is [18]

$$\text{BCRLB} \triangleq (\mathbf{G} + \mathbf{P})^{-1} \tag{36}$$

where $\mathbf{G}$ is the Fisher information matrix averaged with respect to the prior density $\lambda(\boldsymbol{\theta})$

$$\mathbf{G} \triangleq \int \mathbf{F}(\boldsymbol{\theta}) \lambda(\boldsymbol{\theta}) \mathrm{d}\boldsymbol{\theta} \tag{37}$$

and the matrix $\mathbf{P}$ depends only on the prior (and is independent of the aperture matrix). The particular choice of prior does not affect our analysis in the following. By (23), we see that $\mathbf{G}$ can be written as

$$\mathbf{G} = \begin{bmatrix} \mathbf{G}_{\boldsymbol{\theta}_1\boldsymbol{\theta}_1} & \cdots & \mathbf{G}_{\boldsymbol{\theta}_1\boldsymbol{\theta}_L} \\ \vdots & \ddots & \vdots \\ \mathbf{G}_{\boldsymbol{\theta}_L\boldsymbol{\theta}_1} & \cdots & \mathbf{G}_{\boldsymbol{\theta}_L\boldsymbol{\theta}_L} \end{bmatrix} \tag{38}$$

with

$$\mathbf{G}_{\boldsymbol{\theta}_\ell\boldsymbol{\theta}_{\ell'}} \triangleq \int \mathbf{F}_{\boldsymbol{\theta}_\ell\boldsymbol{\theta}_{\ell'}} \lambda(\boldsymbol{\theta}) \mathrm{d}\boldsymbol{\theta}. \tag{39}$$

We remark that the diagonal blocks of $\mathbf{G}$ read

$$\mathbf{G}_{\boldsymbol{\theta}_\ell,\boldsymbol{\theta}_\ell} = \begin{bmatrix} G_{\alpha_\ell\alpha_\ell} & \mathbf{0}^{\mathsf{T}} \\ \mathbf{0} & \mathbf{G}_{\boldsymbol{\vartheta}_\ell\boldsymbol{\vartheta}_\ell} \end{bmatrix} \tag{40}$$

with

$$\mathbf{G}_{\boldsymbol{\vartheta}_\ell\boldsymbol{\vartheta}_\ell} = 8\pi^2 \frac{\mathsf{E}\left[|\alpha_\ell|^2\right] \cdot E}{N_0} \mathbf{A}\mathbf{A}^{\mathsf{T}}, \quad \ell = 1, \ldots, L \tag{41}$$

where $\mathsf{E}\left[|\alpha_\ell|^2\right]$ denotes the expectation with respect to the prior of α_ℓ.

We are now able to give the following characterization of the aperture matrices, which yields the lowest BCRLB in the multipath case.

Theorem 5: Let $\text{BCRLB}_{\tilde{\mathbf{A}}}$ be the BCRLB resulting from the aperture matrix $\tilde{\mathbf{A}}$ and similarly $\text{BCRLB}_{\mathbf{A}}$ the BCRLB resulting from an arbitrary aperture matrix $\mathbf{A}$ with the property that $\operatorname{diag}(\mathbf{A}\mathbf{A}^{\mathsf{T}}) = \operatorname{diag}(\tilde{\mathbf{A}}\tilde{\mathbf{A}}^{\mathsf{T}})$. If the inequality

$$\text{BCRLB}_{\mathbf{A}} \succeq \text{BCRLB}_{\tilde{\mathbf{A}}} \tag{42}$$

is fulfilled for any such aperture matrix $\mathbf{A}$, then the rows of $\tilde{\mathbf{A}}$ are orthogonal.

Proof: We prove Theorem 5 by proving that if the BCRLB of an aperture matrix $\tilde{\mathbf{A}}$ is lower than or equal to the BCRLB of an orthogonal aperture matrix $\mathbf{A}$, then $\tilde{\mathbf{A}}$ is orthogonal as well. By the assumption (42)

$$(\mathbf{G} + \mathbf{P})^{-1} \succeq (\tilde{\mathbf{G}} + \mathbf{P})^{-1} \tag{43}$$

is fulfilled for any $\mathbf{G}$ such that $\operatorname{diag}(\mathbf{A}\mathbf{A}^{\mathsf{T}}) = \operatorname{diag}(\tilde{\mathbf{A}}\tilde{\mathbf{A}}^{\mathsf{T}})$. Making use of (69) in Appendix II and eliminating the $\mathbf{P}$ terms, we obtain from (43)

$$\tilde{\mathbf{G}} \succeq \mathbf{G}. \tag{44}$$

Then, by invoking Lemma 18 in Appendix II and inserting (40), we obtain, after elimination of some irrelevant terms

$$\left[(\mathbf{A}\mathbf{A}^{\mathsf{T}})^{-1}\right]_{p,p} \geq \left[(\tilde{\mathbf{A}}\tilde{\mathbf{A}}^{\mathsf{T}})^{-1}\right]_{p,p}, \quad \text{for all } p. \tag{45}$$

Now, suppose that $\mathbf{A}$ is row-orthogonal. Then $\mathbf{A}\mathbf{A}^{\mathsf{T}}$ is diagonal and $[(\mathbf{A}\mathbf{A}^{\mathsf{T}})^{-1}]_{p,p} = 1/[\mathbf{A}\mathbf{A}^{\mathsf{T}}]_{p,p}$ for all p. Inserting in (45) yields

$$\frac{1}{[(\mathbf{A}\mathbf{A}^{\mathsf{T}})]_{p,p}} \geq \left[(\tilde{\mathbf{A}}\tilde{\mathbf{A}}^{\mathsf{T}})^{-1}\right]_{p,p} \quad \text{for all } p. \tag{46}$$

From [21, Th. 7.7.8], we have that $[(\tilde{\mathbf{A}}\tilde{\mathbf{A}}^{\mathsf{T}})^{-1}]_{p,p} \geq 1/[\tilde{\mathbf{A}}\tilde{\mathbf{A}}^{\mathsf{T}}]_{p,p}$ for any p. Since $\operatorname{diag}(\mathbf{A}\mathbf{A}^{\mathsf{T}}) = \operatorname{diag}(\tilde{\mathbf{A}}\tilde{\mathbf{A}}^{\mathsf{T}})$, then $1/[\mathbf{A}\mathbf{A}^{\mathsf{T}}]_{p,p} = 1/[\tilde{\mathbf{A}}\tilde{\mathbf{A}}^{\mathsf{T}}]_{p,p}$ for any p. Hence $[(\tilde{\mathbf{A}}\tilde{\mathbf{A}}^{\mathsf{T}})^{-1}]_{p,p} \geq 1/[\mathbf{A}\mathbf{A}^{\mathsf{T}}]_{p,p}$ for any p. Combining this additional inequality with (46), we obtain, for any p

$$\frac{1}{[\mathbf{A}\mathbf{A}^{\mathsf{T}}]_{p,p}} \geq \left[(\tilde{\mathbf{A}}\tilde{\mathbf{A}}^{\mathsf{T}})^{-1}\right]_{p,p} \geq \frac{1}{[\mathbf{A}\mathbf{A}^{\mathsf{T}}]_{p,p}} \tag{47}$$

$$\Rightarrow \left[(\tilde{\mathbf{A}}\tilde{\mathbf{A}}^{\mathsf{T}})^{-1}\right]_{p,p} = \frac{1}{[\mathbf{A}\mathbf{A}^{\mathsf{T}}]_{p,p}}. \tag{48}$$

By Lemma 19 in Appendix II, the two inequalities in (47) are fulfilled for all p if and only if $\tilde{\mathbf{A}}\tilde{\mathbf{A}}^{\mathsf{T}}$ is diagonal. Hence, $\tilde{\mathbf{A}}$ is row-orthogonal. ∎

It is worth noticing the difference between Theorems 3 and 5. Theorem 3 states that (in the one-path case) the orthogonality condition (33) is a *necessary and sufficient condition* for the minimum CRLB to be achieved. The result in Theorem 5 states a *necessary* (but not sufficient) condition for an aperture matrix to yield the minimum BCRLB in the sense of (42). The reason for this seemingly weaker result is that the cross-terms $\mathbf{G}_{\ell,\ell'}, \ell \neq \ell'$ in the matrices $\tilde{\mathbf{G}}$ and $\mathbf{G}$ are removed in the step from (44) to (45). If the off-diagonal blocks should be taken into consideration, more specific assumptions must be made about the prior. Considering a prior and a group of apertures such that $\mathbf{G}_{\ell,\ell'} = \mathbf{0}, \ell \neq \ell'$, one can prove that row-orthogonality is a necessary and sufficient condition for an aperture matrix to yield the minimum BCRLB. The proof is similar to that of Theorem 3.

E. Uniform and Parallel Spatiotemporal Apertures

In the following, we define the concept of uniformity of a spatiotemporal aperture matrix and show that uniformity implies that this matrix is row-orthogonal. For convenience we define the row indexes p, q, and r of $\mathbf{A}$ such that $\{p,q,r\} = \{1,2,3\}$ is fulfilled. Let $\mathbf{b}$ be a column of $\mathbf{A}$, i.e., $\mathbf{b} \in \{\mathbf{a}_1, \ldots, \mathbf{a}_I\}$. Then the number of columns of $\mathbf{A}$ that coincide with $\mathbf{b}$ in the pth and qth elements can be written as

$$\varphi_{p,q}(\mathbf{b}) \triangleq \left|\{i \in \{1,\ldots,I\} : ([\mathbf{b}]_p, [\mathbf{b}]_q) = ([\mathbf{a}_i]_p, [\mathbf{a}_i]_q)\}\right|.$$

Definition 6: A spatiotemporal aperture matrix $\mathbf{A}$ is (p,q)-*uniform* if and only if there exists a constant $\varphi_{p,q}$ such that $\varphi_{p,q}(\mathbf{b}) = \varphi_{p,q}$, for all $\mathbf{b} \in \{\mathbf{a}_1, \ldots, \mathbf{a}_I\}$.

We can now prove a simple lemma that turns out to be helpful for the design of row-orthogonal spatiotemporal aperture matrices.

Lemma 7: Row p and row q of a (p,q)-uniform spatiotemporal aperture matrix $\mathbf{A}$ are orthogonal.

Proof: Let $\mathbf{c}_r^{\mathsf{T}} = [c_{r,1}, \ldots, c_{r,I}]$ denote the rth row of $\mathbf{A}$ and $\mathcal{C}_r = \bigcup_{i=1}^{I} \{c_{r,i}\}$. Then $\sum_{i=1}^{I} c_{p,i} = \varphi_{p,q}|\mathcal{C}_q| \sum_{c_p \in \mathcal{C}_p} c_p$. Therefore

$$\mathbf{c}_q^{\mathsf{T}}\mathbf{c}_p = \sum_{i=1}^{I} c_{q,i}c_{p,i} = \varphi_{p,q} \sum_{c_q \in \mathcal{C}_q} c_q \sum_{c_p \in \mathcal{C}_p} c_p.$$

By convention $\sum_{i=1}^{I} c_{p,i} = 0$, which implies $\sum_{c_p \in \mathcal{C}_p} c_p = 0$. Thus $\mathbf{c}_q^{\mathsf{T}}\mathbf{c}_p = 0$. ∎

As an example, a (2,3)-uniform (i.e., *spatially uniform*) aperture is a spatiotemporal aperture where all pairs of antenna array elements (m_1, m_2) are active $\varphi_{2,3}$ times during one measurement run. For all spatially uniform aperture matrices, the condition $\mathbf{d}_1^{\mathsf{T}}\mathbf{d}_2 = 0$ is fulfilled. For instance, the spatiotemporal aperture matrix defined by (34) and (35) is spatially uniform with $\varphi_{2,3} = 1$ and, therefore, $\mathbf{d}_1^{\mathsf{T}}\mathbf{d}_2 = 0$ in this case.

For a parallel sounding system with M_1 transmitters and M_2 receivers where all antenna pairs are active simultaneously, we see that $I = JM_1M_2$. In this case, $\mathbf{A}$ is (1,2)-uniform with $\varphi_{1,2} = M_2$, $(1,3)$-uniform with $\varphi_{1,3} = M_1$ and (2,3)-uniform with $\varphi_{2,3} = J$. Therefore, such a system always fulfills (33). This result agrees with that in [22] and [23], that $[\mathbf{F}_{\boldsymbol{\vartheta}_\ell\boldsymbol{\vartheta}_\ell}]_{1,3} = [\mathbf{F}_{\boldsymbol{\vartheta}_\ell\boldsymbol{\vartheta}_\ell}]_{3,1} = 0$ always hold for a parallel system with $M_1 = 1$.

From the observation that parallel systems always fulfill (33), it might seem tempting to conclude that parallel systems are preferable to switched systems. However, the comparison of the CRLBs of different spatiotemporal apertures must be done with the same SNR and thus with the same I for all considered apertures. To illustrate the comparison problem, we consider the case where all antenna pairs are active once during the measurement run. In a parallel system, this condition implies that all samples are taken simultaneously and therefore $|\mathbf{t}|^2 = 0$. Hence, in this case, Doppler frequency estimation is not possible. In a switched sounding system, the same condition implies that $|\mathbf{t}|^2 > 0$, and thus a spatiotemporal aperture with finite CRLB can be constructed. In general, one can always construct a spatiotemporal aperture of a switched sounding system with a value $|\mathbf{t}|^2$ larger than that of a parallel sounding system with the same number of samples. An additional major difference between parallel and switched systems is that parallel systems do not allow for adjustments of $|\mathbf{d}_k|^2$ without changing the geometry of the antenna arrays, as do switched systems.

IV. Spatiotemporal Ambiguity Function

In this section, we define a (bi)spatiotemporal ambiguity function for channel sounding. To our best knowledge, this problem has not previously been addressed in published work.

Definition 8: The *Doppler-(bi)direction ambiguity function* of a (bi)spatiotemporal channel sounding system is defined to be

$$\chi(\boldsymbol{\vartheta}, \bar{\boldsymbol{\vartheta}}) \triangleq \frac{1}{EI\alpha^*\bar{\alpha}} \sum_{i=1}^{I} \int_{\mathcal{T}_{j(i)}} s_i^*(t;\boldsymbol{\theta}) s_i(t;\bar{\boldsymbol{\theta}}) \mathrm{d}t \tag{49}$$

where $s_i(t;\boldsymbol{\theta}) \triangleq s_{j(i),m_1(i),m_2(i)}(t;\boldsymbol{\theta})$ with $s_{j,m_1,m_2}(t;\boldsymbol{\theta})$ defined in (5).

The magnitude of the ambiguity function ranges from zero to unity. For any $\boldsymbol{\vartheta} \in \mathcal{E}_{\boldsymbol{\vartheta}}$, $|\chi(\boldsymbol{\vartheta},\boldsymbol{\vartheta})| = 1$. In the case where there exists a vector $\bar{\boldsymbol{\vartheta}} \in \mathcal{E}_{\boldsymbol{\vartheta}}, \bar{\boldsymbol{\vartheta}} \neq \boldsymbol{\vartheta}$ such that $|\chi(\boldsymbol{\vartheta},\bar{\boldsymbol{\vartheta}})| = 1$, two signal components with parameter vectors $\boldsymbol{\vartheta}$ and $\bar{\boldsymbol{\vartheta}}$, respectively, are indistinguishable. We call this the ambiguity effect. Due to the particular form of the sounding pulses [see, e.g., (5)], the ambiguity function in (49) can be recast as

$$\chi(\boldsymbol{\vartheta},\bar{\boldsymbol{\vartheta}}) = \frac{1}{I}\sum_{i=1}^{I} \exp(-j2\pi(\boldsymbol{\vartheta}-\bar{\boldsymbol{\vartheta}})^{\mathsf{T}}\mathbf{a}_i)\cdot \mathrm{EF_n}(\nu-\bar{\nu};i). \quad (50)$$

Thus, $\chi(\boldsymbol{\vartheta},\bar{\boldsymbol{\vartheta}})$ is a function of the difference vector $\boldsymbol{\vartheta}-\bar{\boldsymbol{\vartheta}}$, i.e., $\chi(\boldsymbol{\vartheta},\bar{\boldsymbol{\vartheta}}) = \chi_0(\boldsymbol{\vartheta}-\bar{\boldsymbol{\vartheta}})$. For simplicity, we refer to both $\chi(\boldsymbol{\vartheta},\bar{\boldsymbol{\vartheta}})$ and $\chi_0(\boldsymbol{\vartheta})$ as "ambiguity function." It suffices to investigate the behavior of $\chi_0(\boldsymbol{\vartheta})$, defined as

$$\chi_0(\boldsymbol{\vartheta}) = \chi(\boldsymbol{\vartheta},\mathbf{0}) \quad (51)$$

$$= \frac{1}{I}\sum_{i=1}^{I} \exp(-j2\pi\boldsymbol{\vartheta}^{\mathsf{T}}\mathbf{a}_i)\cdot \mathrm{EF_n}(\nu;i). \quad (52)$$

Notice that while the definition of Woodward's ambiguity function [8] involves the transmitted signal only, the definition (49) includes both the transmitted temporal signal and the spatial aperture. A more general class of ambiguity functions is derived in [9], where the definition given in (49) is a special case. It is shown in Appendix III that the Doppler-direction ambiguity function fulfills a constant volume property, as does Woodward's ambiguity function. Due to this property, ambiguity volume can be moved from one region of the estimation range to another but not canceled. Thus, if a side-lobe of the ambiguity function is suppressed, the corresponding suppressed ambiguity volume appears elsewhere.

Inspired by the terminology used in antenna theory [24], we call $\mathrm{EF_n}(\nu;i)$ the *normalized element factor* of the sounding pulse i. When all element factors are equal, i.e., $\mathrm{EF_n}(\nu;i) = \mathrm{EF_n}(\nu)$, the ambiguity function simplifies to

$$\chi_0(\boldsymbol{\vartheta}) = \mathrm{EF_n}(\nu)\cdot \mathrm{AF_n}(\boldsymbol{\vartheta};\mathbf{A}) \quad (53)$$

where

$$\mathrm{AF_n}(\boldsymbol{\vartheta};\mathbf{A}) \triangleq \frac{1}{I}\sum_{i=1}^{I} \exp(-j2\pi\boldsymbol{\vartheta}^{\mathsf{T}}\mathbf{a}_i) \quad (54)$$

is the *normalized spatiotemporal array factor* or array factor, for short. The factorization of (53) is analogous to the well-known factorization in the theory of antenna systems. The radiation pattern of an antenna array with identical elements is the product of an element factor and an array factor [24]. This factorization splits the impacts on the ambiguity function of the array elements, reflected via the element factor, and of the aperture configuration, reflected via the array factor. The main concern of this paper is the impact of the configuration of the spatiotemporal aperture of an MIMO channel sounder. Thus, the factor of interest in the product (53) is the array factor. Two equivalent conceptual approaches can be followed to investigate the effect of the aperture configuration only. The first approach consists merely in restricting the attention to the array factor of the aperture. The second approach consists in considering an ambiguity function induced by the aperture with the impact of the element factor dropped. This is achieved by assuming that the element factor is constant. This assumption is often valid since the duration of a measurement run is typically large compared to the duration of a sounding pulse. The fact that both conceptual approaches are equivalent follows from (53).

It follows from (54) that the array factor achieves its maximum value at $\boldsymbol{\vartheta} = \mathbf{0}$, namely, $|\mathrm{AF_n}(\mathbf{0};\mathbf{A})| = 1$. If there exists a nonzero $\boldsymbol{\vartheta} \in \mathcal{E}_{\boldsymbol{\vartheta}}$ such that $|\mathrm{AF_n}(\boldsymbol{\vartheta};\mathbf{A})| = 1$ is fulfilled, the ambiguity effect occurs, provided that the element factor is constant. This observation leads to the following definition.

Definition 9 (Ambiguous Array Factor): A spatiotemporal array factor $\mathrm{AF_n}(\boldsymbol{\vartheta};\mathbf{A})$ is ambiguous if there exists a $\boldsymbol{\vartheta} \neq \mathbf{0}$ in $\mathcal{E}_{\boldsymbol{\vartheta}}$ such that $|\mathrm{AF_n}(\boldsymbol{\vartheta};\mathbf{A})| = 1$.

A spatiotemporal array factor that is not ambiguous is termed a *nonambiguous array factor*. If a spatiotemporal aperture yields an ambiguous array factor, we say *the aperture is ambiguous*.

In the following, we analyze how the spatiotemporal aperture affects the array factor. In particular, we state a necessary and sufficient condition for a spatiotemporal aperture to be ambiguous.

A. Specific Examples (Continued)

The following numerical examples illustrate the behavior of the array factor for different spatiotemporal apertures. We consider an SIMO-ULA system with $I = 64$ and $M_2 = 8$. Fig. 3 reports the magnitude of the array factors corresponding to four different spatiotemporal apertures for $(\nu,\omega_2) \in -(1/(2T_r),+1/(2T_r)] \times (-1,+1]$. In Fig. 3(a), $m_2(i)$ is given by (35). It is apparent from the figure that the absolute value of the array factor exhibits multiple maxima of unit magnitude and is therefore ambiguous. In Fig. 3(b), $m_2(i)$ is defined by $m_2(i) = \lceil i/8 \rceil$, i.e., each Array 2 element is active eight times in succession. As shown in Fig. 3(b), this yields a nonambiguous array factor with a unique maximum but a wide main-lobe. Hence high variances of $\hat{\nu}$ and $\hat{\omega}_2$ are to be expected in this case at large SNRs. Furthermore, since the main-lobe is tilted, an error in the Doppler frequency estimate affects the error in the direction estimate and vice-versa. The two estimators are statistically dependent. In Fig. 3(c), $\mathbf{m}_2$ is defined by $\mathbf{m}_2 = \mathbf{1}_8 \otimes [3,2,7,1,5,8,6,4]^{\mathsf{T}}$. This spatial array corresponds to permuting the array element indices and then applying the spatial sounding given in (35). It is apparent from Fig. 3(c) that the array factor is nonambiguous in this case, and its main lobe is narrower than that depicted in Fig. 3(b). However, "stripes" of side-lobes separated by $1/8$ along the νT_r axis are visible. Finally, Fig. 3(d) depicts the array factor when $\mathbf{m}_2$ results from a random permutation of the vector $\mathbf{1}_8 \otimes [1,2,\ldots,8]^{\mathsf{T}}$. The depicted function has a unique maximum and the magnitude of the highest side-lobe is significantly lower than in Fig. 3(c).

Due to the factorization (53), the constant volume property of the ambiguity function is fulfilled for the array factor as well. This effect is clearly visible in Fig. 3(a)–(d). In Fig. 3(a), the ambiguity volume is concentrated in eight lobes with unit maximum magnitude. Thus, the array factor depicted in Fig. 3(a)

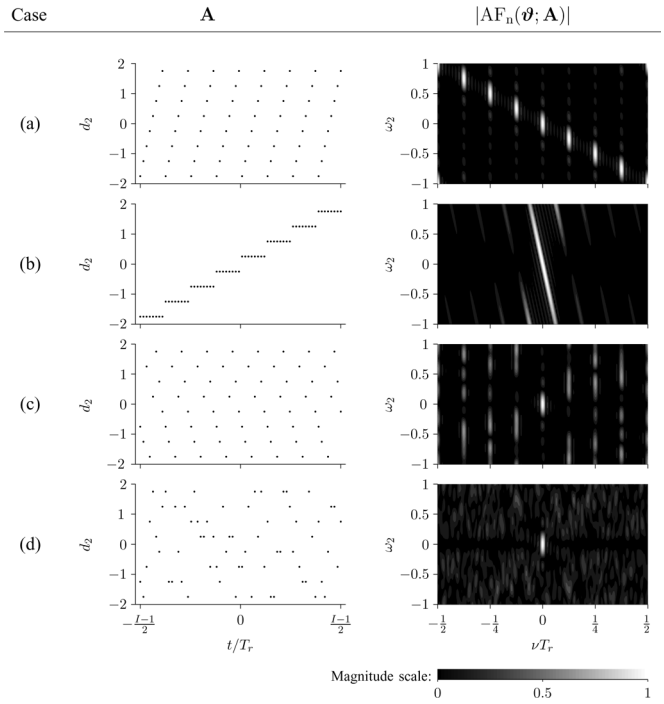

Fig. 3. The spatiotemporal arrays (left plots) and corresponding magnitude of the array factors (right plots) in the four cases (a)–(d) described in the text. Each dot of the aperture plots denotes one $(t(i), d_2(i))$ point, i.e., the centroid of one spatiotemporal sample.

is ambiguous. In Fig. 3(b), the volume is mainly located in the wide main-lobe. In Fig. 3(c) the volume is concentrated in the main-lobe and in stripes of side-lobes. In Fig. 3(d), there is no large side-lobe, and the main-lobe remains rather narrow. Instead, the ambiguity volume is distributed to the multiple small-magnitude side-lobes.

B. Necessary and Sufficient Condition for a Spatiotemporal Aperture to be Ambiguous

The following lemma gives a necessary and sufficient condition for a spatiotemporal aperture to be ambiguous.

Lemma 10: A spatiotemporal aperture is ambiguous if and only if there exists $\boldsymbol{\vartheta} \in \mathcal{E}_{\boldsymbol{\vartheta}}$, $\boldsymbol{\vartheta} \neq \mathbf{0}$, such that

$$(\mathbf{a}_i - \mathbf{a}_{i+1})^{\mathsf{T}} \boldsymbol{\vartheta} \equiv 0 \bmod 1, \quad i = 1, \ldots, I-1. \tag{55}$$

Proof: The spatiotemporal array factor $\mathrm{AF_n}(\boldsymbol{\vartheta};\mathbf{A})$ has magnitude of one if and only if the phases of the exponential terms in (54) satisfy

$$2\pi \mathbf{a}_1^{\mathsf{T}} \boldsymbol{\vartheta} \equiv 2\pi \mathbf{a}_2^{\mathsf{T}} \boldsymbol{\vartheta} \equiv \cdots \equiv 2\pi \mathbf{a}_I^{\mathsf{T}} \boldsymbol{\vartheta} \bmod 2\pi. \tag{56}$$

The total number of congruences in this system is the factorial of I. Solving (56) is equivalent to solving the $I-1$ "neighboring" congruences (55). The latter set of congruences is always fulfilled for the "trivial solution" $\boldsymbol{\vartheta} = \mathbf{0}$. The array factor $\mathrm{AF_n}(\boldsymbol{\vartheta};\mathbf{A})$ is ambiguous if, and only if, (56) has a nontrivial solution ($\boldsymbol{\vartheta} \neq \mathbf{0}$) in $\mathcal{E}_{\boldsymbol{\vartheta}}$. ■

C. Specific Examples (Continued)

In the following, we define a class of spatiotemporal apertures for an SIMO-ULA system called modulo-type apertures and show that the elements in this class are ambiguous.

Definition 11: A *modulo-type spatiotemporal aperture* of an SIMO-ULA system is an aperture satisfying

$$m_2(i) = (iK_a + K_b \bmod M_2) + 1 \tag{57}$$

where $K_a, K_b \in \mathbb{Z}$ are relatively prime.

As an example, the commonly used spatiotemporal aperture given in (35) is a modulo-type aperture with $K_a = 1$ and $K_b = -1$.

For an SIMO-ULA system, (55) reads

$$-\nu T_r + (d_2(i) - d_2(i+1))\omega_2 \equiv 0 \bmod 1 \quad \text{for all } i \in \{1, \ldots, I-1\}. \tag{58}$$

It is easy to see that for a modulo-type aperture, $m_2(i) - m_2(i+1) \in \{-K_a, M_2 - K_a\}$, for all $i \in \{1, \ldots, I-1\}$. Therefore, by inserting (57) in (58), we obtain the congruences

$$\nu T_r + \frac{\omega_2}{2} K_a \equiv 0 \bmod 1, \text{ and } \frac{\omega_2}{2} M_2 \equiv 0 \bmod 1. \tag{59}$$

Solving for $(\nu T_r, \omega_2) \in (-(1/2), (1/2)] \times (-1, 1]$ yields the system of equations

$$\begin{aligned} \omega_2 &= \frac{2n_a}{M_2}, \quad n_a \in \mathbb{Z} \cap \left(-\frac{M_2}{2}, \frac{M_2}{2}\right], \text{ and} \\ \nu T_r &= -K_a \frac{n_a}{M_2} + n_b, \\ n_b &\in \left\{ k \in \mathbb{Z} : \nu T_r \in \left(-\frac{1}{2}, \frac{1}{2}\right] \right\}. \end{aligned} \tag{60}$$

It can be seen that for each n_a, there exists a unique n_b satisfying (60) such that (56) holds. Therefore, there exist in total M_2 different pairs $(\nu T_r, \omega_2) \in (-1/2, 1/2] \times (-1, 1]$ such that (56) is fulfilled. Thus, any modulo-type spatiotemporal aperture of an SIMO-ULA system is ambiguous. As remarked in Section IV-A, this effect is clearly visible in Fig. 3(a), where the array factor exhibits $M_2 = 8$ different lobes of unit magnitude at the positions $(\nu T_r, \omega_2) = (-n_a/8, n_a/4), n_a = -3, -2, \ldots, +4$.

D. Component Apertures and Subapertures

It is, in general, difficult to prove whether, for a given spatiotemporal aperture, the system of congruences (55) is fulfilled or not. However, in the following, we give the definition of the two concepts of "component aperture" and "subaperture" and show two corollaries of Lemma 10 that are useful for identifying ambiguous apertures.

Definition 12 (Component Aperture): Let $\mathbf{A}$ be a spatiotemporal aperture matrix. Then the aperture matrix $\tilde{\mathbf{A}}$ of a component aperture is obtained by replacing one or two rows of $\mathbf{A}$ by the all-zero row.

Definition 13 (Subaperture): Let $\mathbf{A}$ be spatiotemporal aperture matrix. Then the aperture matrix of a subaperture is obtained by erasing a number of columns in $\mathbf{A}$.

Inserting Definition 12 in Lemma 10 yields the corollary.

Corollary 14: A spatiotemporal aperture with one ambiguous component aperture is ambiguous.

Corollary 15: Any subaperture of an ambiguous aperture is ambiguous.

Proof: The proof follows from the observation that if (56) is fulfilled, then a subset of the congruences is fulfilled as well. Therefore, if (56) is fulfilled for $\mathbf{A}$, it is fulfilled for $\tilde{\mathbf{A}}$ too. ■

As an example of Corollary 14, a *sufficient* condition for an aperture of a MIMO-ULA system to be ambiguous is that either $\mathbf{m}_1$ or $\mathbf{m}_2$ yields an ambiguous array factor when used in an SIMO-ULA system. Therefore if a modulo-type aperture is used at either the transmitter or the receiver in a MIMO-ULA system, the corresponding array factor is ambiguous. It is worth noting that the most commonly used spatiotemporal apertures are indeed formed by a combination of a repetition scheme [as the one used in Fig. 3(b)] at Array 1 and a modulo-type scheme at the Array 2. Since in this case the component aperture formed by the temporal aperture and the spatial aperture at Array 2 is ambiguous, the whole bispatiotemporal aperture is ambiguous.

We see by Corollary 15 and the example given in Section IV-C that any aperture formed by leaving out sounding pulse of a modulo-type aperture is ambiguous. One such aperture was analyzed in [5].

V. The Impact of the Spatiotemporal Aperture on the Threshold Effect

In the following, we investigate the effect of the spatiotemporal aperture on the root mean-squared estimation error (rmsee) of the joint Doppler frequency and spatial frequency estimator. We consider the one-path case ($L = 1$). To simplify the notation, we drop the path index $\ell = 1$ in the sequel.

Generally, the rmsee of a nonlinear estimator exhibits the same typical behavior that we sketch here considering the parameter vector $\boldsymbol{\vartheta}$. Below a certain threshold $\gamma_{\mathrm{o},[\hat{\boldsymbol{\vartheta}}]_p}^{\mathrm{th}}$ in SNR, the rmsee of $[\hat{\boldsymbol{\vartheta}}]_p$ increases rapidly as the SNR decreases [25], [26]. This effect is commonly known as the *threshold effect*. The previous sections show that the spatiotemporal aperture determines the behavior of the array factor $\mathrm{AF_n}(\boldsymbol{\vartheta};\mathbf{A})$ and therefore of the ambiguity function $\chi_0(\boldsymbol{\vartheta})$. As can be seen from the examples given in Section IV-A, the magnitudes of the side-lobes of the array factor depend on the spatiotemporal aperture. Consequently, the spatiotemporal aperture also affects the robustness of the estimators toward noise, since this robustness directly depends on the magnitudes of the side-lobes [25]. In the following, we use the NSL associated with a spatiotemporal aperture as a figure of merit for noise robustness of the parameter estimators.

Definition 16: The NSL associated with a spatiotemporal aperture matrix $\mathbf{A}$ is defined as

$$\mathrm{NSL}(\mathbf{A}) \triangleq \max_{\boldsymbol{\vartheta}\in\mathcal{L}} |\mathrm{AF_n}(\boldsymbol{\vartheta};\mathbf{A})| \tag{61}$$

where $\mathcal{L} \triangleq \{\boldsymbol{\vartheta} \in \mathcal{E}_{\boldsymbol{\vartheta}} : (\partial/\partial\boldsymbol{\vartheta})\mathrm{AF_n}(\boldsymbol{\vartheta};\mathbf{A}) = \mathbf{0}, \boldsymbol{\vartheta} \neq \mathbf{0}\}$ is the set of local maxima of $|\mathrm{AF_n}(\boldsymbol{\vartheta};\mathbf{A})|, \boldsymbol{\vartheta} \in \mathcal{E}_{\boldsymbol{\vartheta}}$.

If a spatiotemporal aperture is ambiguous there exists by definition at least one $\boldsymbol{\vartheta} \neq \mathbf{0}$ such that $|\mathrm{AF_n}(\boldsymbol{\vartheta};\mathbf{A})| = 1$ and therefore NSL$= 1$. On the contrary, a spatiotemporal aperture with NSL less than one has a unique maximum. In that case, the NSL coincides with the magnitude of the highest side-lobe of the normalized array factor. Generally, the NSL is hard to obtain analytically but can, however, be computed numerically.

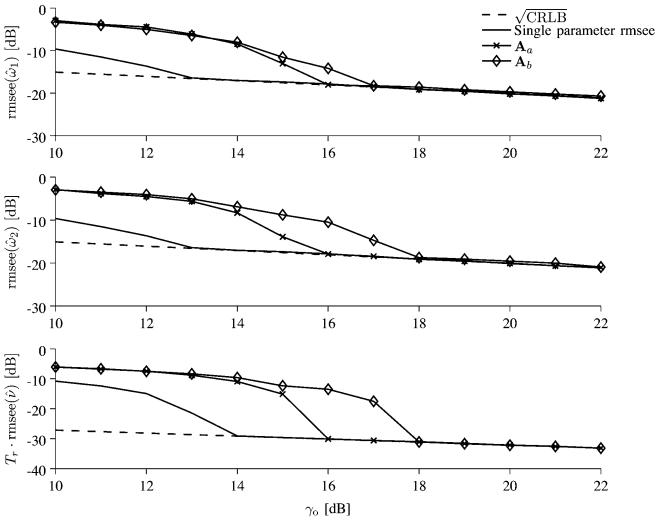

Fig. 4. Simulated rmsee curves obtained from 1000 Monte Carlo runs using the two different orthogonal spatiotemporal apertures $\mathbf{A}_a$ (marked with $\times$) and $\mathbf{A}_b$ (marked with $\diamond$). The dashed lines are the corresponding CRLBs obtained from (32). The solid curves without marks show the simulated rmsee of the single-parameter maximum-likelihood estimator with all other parameters known. An MIMO-ULA type system with $M_1 = M_2 = 8$ and $I = 64$ is used and $\boldsymbol{\vartheta}_1 = \mathbf{0}$. Isotropic sounding pulses are assumed ($\mathrm{EF_n}(\boldsymbol{\vartheta}) = 1$).

To study the relation between the NSL and $\gamma_{\mathrm{o}}^{\mathrm{th}}$ in more detail, a method for computing $\gamma_{\mathrm{o}}^{\mathrm{th}}$ is needed. Motivated by the observation that the estimators at hand all converge to the CRLB at high SNR, $\gamma_{\mathrm{o},[\hat{\boldsymbol{\vartheta}}]_p}^{\mathrm{th}}$ is defined in the following as the maximum γ_{o} such that the inequality:

$$\mathrm{rmsee}([\hat{\boldsymbol{\vartheta}}]_p) \leq 2\sqrt{\mathrm{CRLB}([\hat{\boldsymbol{\vartheta}}]_p)} \tag{62}$$

is fulfilled. The threshold $\gamma_{\mathrm{o}}^{\mathrm{th}}$ of the joint estimator $\hat{\boldsymbol{\vartheta}}$ is defined as the maximum of the thresholds of the individual estimators $\hat{\nu}$, $\hat{\omega}_1$, and $\hat{\omega}_2$, i.e.,

$$\gamma_{\mathrm{o}}^{\mathrm{th}} \triangleq \max\left\{\gamma_{\mathrm{o},\hat{\nu}}^{\mathrm{th}}, \gamma_{\mathrm{o},\hat{\omega}_1}^{\mathrm{th}}, \gamma_{\mathrm{o},\hat{\omega}_2}^{\mathrm{th}}\right\}. \tag{63}$$

Hence, $\gamma_{\mathrm{o}}^{\mathrm{th}}$ can be determined if the rmsee is known. In practice, the rmsee and $\hat{\gamma}_{\mathrm{o}}^{\mathrm{th}}$ are estimated by means of Monte Carlo simulations.

A. Specific Examples (Continued)

Fig. 4 reports the results of a Monte Carlo simulation comparing the rmsees of $\hat{\nu}$, $\hat{\omega}_1$, and $\hat{\omega}_2$ using two different orthogonal spatiotemporal aperture matrices $\mathbf{A}_a$, with $\mathrm{NSL}(\mathbf{A}_a) = 0.50$, and $\mathbf{A}_b$, with $\mathrm{NSL}(\mathbf{A}_b) = 0.63$ together with the corresponding CRLBs. The parameter setting used for this simulation is reported in the caption of the figure. For comparison, we have included the simulated rmsee of each single maximum likelihood estimator of ν, ω_1, and ω_2 with the two other parameters known. These curves are lower bounds on the rmsees when all parameters are estimated jointly.

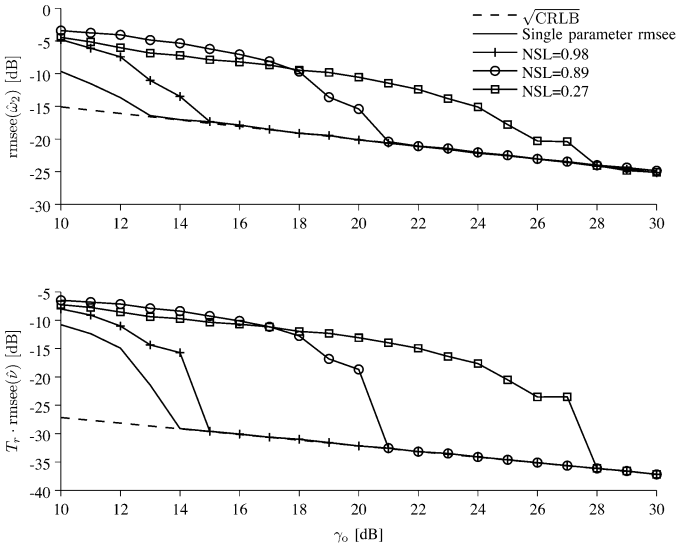

Fig. 5. Simulated rmsee versus SNR for an SIMO-ULA system with settings $M_1 = 1$, $M_2 = 8$, and $I = 64$. The remaining settings are the same as those reported in the caption of Fig. 4. The resulting rmsees of three spatiotemporal apertures with different NSLs are plotted. The dashed lines are the corresponding CRLBs. The solid curves without marks show the rmsees of the single-parameter maximum likelihood estimators when all other parameters are known.

In the $\mathbf{A}_a$ case, the threshold estimates $\hat{\gamma}_{\mathrm{o},\hat{\nu}}^{\mathrm{th}}$, $\hat{\gamma}_{\mathrm{o},\hat{\omega}_1}^{\mathrm{th}}$, and $\hat{\gamma}_{\mathrm{o},\hat{\omega}_2}^{\mathrm{th}}$ all take the value 16 dB; hence

$$\hat{\gamma}_{\mathrm{o}}^{\mathrm{th}} \triangleq \max\left\{\hat{\gamma}_{\mathrm{o},\hat{\nu}}^{\mathrm{th}}, \hat{\gamma}_{\mathrm{o},\hat{\omega}_1}^{\mathrm{th}}, \hat{\gamma}_{\mathrm{o},\hat{\omega}_2}^{\mathrm{th}}\right\} = 16\ \mathrm{dB} \tag{64}$$

for $\mathbf{A}_b$, the estimated threshold values are $\hat{\gamma}_{\mathrm{o},\hat{\nu}}^{\mathrm{th}} = \hat{\gamma}_{\mathrm{o},\hat{\omega}_1}^{\mathrm{th}} = 18\,\mathrm{dB}$, $\hat{\gamma}_{\mathrm{o},\hat{\omega}_2}^{\mathrm{th}} = 17\,\mathrm{dB}$ and, consequently, $\hat{\gamma}_{\mathrm{o}}^{\mathrm{th}} = 18\,\mathrm{dB}$. Defining $\hat{\gamma}_{\mathrm{o,single}}^{\mathrm{th}}$ as the largest threshold estimate for the single-parameter estimators, we see that $\hat{\gamma}_{\mathrm{o}}^{\mathrm{th}}$ exceeds $\hat{\gamma}_{\mathrm{o,single}}^{\mathrm{th}}$ by 2 and 4 dB in the $\mathbf{A}_a$ and $\mathbf{A}_b$ cases, respectively. The simulation results given in Fig. 4 suggest that one should select an orthogonal spatiotemporal aperture matrix that yields the lowest possible $\gamma_{\mathrm{o}}^{\mathrm{th}}$.

We now consider an SIMO-ULA system and assume that ω_1 is known. We consider three spatiotemporal apertures with NSL$= 0.27, 0.89$, and 0.98, respectively. The simulated rmsees together with the corresponding CRLBs and the simulated single-parameter rmsees are reported in Fig. 5. As can be observed from the figure, $\hat{\gamma}_{\mathrm{o}}^{\mathrm{th}}$ increases with the NSL. In the NSL$=0.27$ case, $\hat{\gamma}_{\mathrm{o}}^{\mathrm{th}}$ exceeds $\hat{\gamma}_{\mathrm{o,single}}^{\mathrm{th}}$ by approximately 1 dB.

In the above investigation, a very large number of Monte Carlo runs is required to estimate the threshold position accurately. Therefore, this approach is not feasible when a large number of spatiotemporal aperture matrices should be compared. Furthermore, the Monte Carlo simulations commonly underestimate $\gamma_{\mathrm{o}}^{\mathrm{th}}$ due to the low outlier probability [27]. Hence the $\hat{\gamma}_{\mathrm{o}}^{\mathrm{th}}$ values obtained from Figs. 4 and 5 are too optimistic. Several methods for estimating the threshold value of an estimator are available in the literature. In [28], [29], Athley describes a method to approximate the rmsee in the threshold region based on the magnitudes of the side-lobes of the ambiguity function.

Fig. 6 reports $\hat{\gamma}_{\mathrm{o}}^{\mathrm{th}}$ for different selections of $\mathbf{A}$ as a function of the corresponding NSL. The parameter settings are the same as

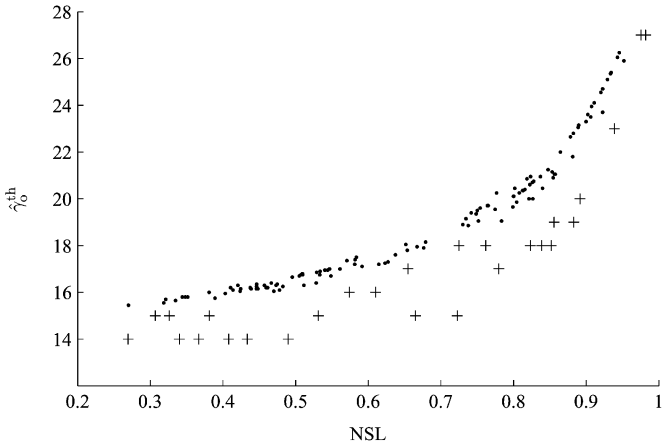

Fig. 6. The estimated rmsee threshold $\hat{\gamma}_{\mathrm{o}}^{\mathrm{th}}$ as a function of the NSL. The points marked by • are obtained from Athley's method, while the points marked with + are obtained from Monte Carlo simulations. The simulation setting is described in the caption of Fig. 5.

in Fig. 5. The points marked by "•" are obtained using Athley's method [28, eq. (20)]; the points marked "+" are obtained from Monte Carlo simulations with 1000 runs and varying γ_{o} in steps of 1 dB. It is apparent from the figure that the values of $\hat{\gamma}_{\mathrm{o}}^{\mathrm{th}}$ obtained from the Monte Carlo simulations are maximally 4 dB lower than the $\hat{\gamma}_{\mathrm{o}}^{\mathrm{th}}$ values obtained using Athley's method. This is to be expected due to the finite number of Monte Carlo runs and the uncertainty caused by the 1 dB quantization of γ_{o} used in the simulation. As can be seen for both methods, the obtained estimates $\hat{\gamma}_{\mathrm{o}}^{\mathrm{th}}$ exhibit an increasing trend with respect to the NSL. Hence, the NSL can be used as a figure of merit to assess the robustness of spatiotemporal aperture towards noise.

VI. Conclusion

A novel model of wireless MIMO channel sounding systems was proposed. This model is based on the concept of (bi)spatiotemporal aperture and can describe switched as well as parallel sounding systems. The proposed model provides a description of the impact of spatiotemporal sounding on the joint estimation of Doppler frequency, direction of arrival, and direction of departure. The Fisher information matrix and the conditional CRLBs on the estimator variances were derived. For the one-path case, it was shown analytically that a spatiotemporal aperture fulfilling an orthogonality property yields the minimum CRLBs. It was also shown that the aperture which yields the minimum Bayesian CRLB in the multipath case also fulfills this orthogonality criterion.

An ambiguity function for Doppler-bidirection estimation was defined. The ambiguity function factorizes into an "element factor" multiplied by an "array factor" The necessary and sufficient condition for the array factor to be ambiguous was stated, and a certain family of spatiotemporal apertures (the so-called modulo-type apertures), which includes the most commonly used apertures, was found to be ambiguous, i.e., to yield an ambiguous array factor.

Monte Carlo simulations show that the normalized side-lobe level is a sensible figure of merit for the identification of spatiotemporal apertures performing close to optimum in terms of

root mean square estimation error among the class of spatiotemporal apertures exhibiting the orthogonality property.

As a general conclusion, when designing a spatiotemporal aperture for joint estimation of Doppler frequency, direction of departure, and direction of arrival, it is not advisable to optimize the temporal or spatial apertures separately. Joint optimization of the bispatiotemporal aperture should be performed instead.

Appendix I
Derivation of the Conditional Fisher Information Matrix

The Fisher information matrix $\mathbf{F}(\boldsymbol{\theta})$ for joint estimation of the parameter vector $\boldsymbol{\theta} = \left[\boldsymbol{\theta}_1^{\mathsf{T}}, \ldots, \boldsymbol{\theta}_L^{\mathsf{T}}\right]^{\mathsf{T}}$ from an observation of $Y_1(t), \ldots, Y_I(t)$ can be written as

$$\mathbf{F}(\boldsymbol{\theta}) \triangleq \begin{bmatrix} \mathbf{F}_{\boldsymbol{\theta}_1\boldsymbol{\theta}_1} & \cdots & \mathbf{F}_{\boldsymbol{\theta}_1\boldsymbol{\theta}_L} \\ \vdots & \ddots & \vdots \\ \mathbf{F}_{\boldsymbol{\theta}_L\boldsymbol{\theta}_1} & \cdots & \mathbf{F}_{\boldsymbol{\theta}_L\boldsymbol{\theta}_L} \end{bmatrix} \tag{65}$$

where we use the notation

$$\mathbf{F}_{\boldsymbol{\beta}\boldsymbol{\xi}} \triangleq -\mathsf{E}\left[\frac{\partial}{\partial \boldsymbol{\beta}}\Lambda(\boldsymbol{\theta})\frac{\partial}{\partial \boldsymbol{\xi}^{\mathsf{H}}}\Lambda(\boldsymbol{\theta})\right] \tag{66}$$

with the complex gradient defined as in [30, Appendix B]. We remark that in (66), the explicit mention of the dependence of $\boldsymbol{\theta}$ has been dropped to simplify the notation. Using [2], (22), $\mathbf{F}_{\boldsymbol{\theta}_\ell\boldsymbol{\theta}_{\ell'}}$ can be rewritten as

$$\begin{aligned}\mathbf{F}_{\boldsymbol{\theta}_\ell\boldsymbol{\theta}_{\ell'}} &= \frac{2}{N_0}\Re\left\{\int_{\mathcal{T}_0}\sum_{i=1}^{I}\frac{\partial s_i(t,\boldsymbol{\theta})}{\partial \boldsymbol{\theta}_\ell}\cdot\frac{\partial s_i^*(t,\boldsymbol{\theta})}{\partial \boldsymbol{\theta}_{\ell'}{}^{\mathsf{H}}}\,\mathrm{d}t\right\} \\ &= \frac{2}{N_0}\Re\left\{\sum_{i=1}^{I}\int_{\mathcal{T}_{j(i)}}\frac{\partial s_i(t;\boldsymbol{\theta}_\ell)}{\partial \boldsymbol{\theta}_\ell}\cdot\frac{\partial s_i^*(t;\boldsymbol{\theta}_{\ell'})}{\partial \boldsymbol{\theta}_{\ell'}{}^{\mathsf{H}}}\mathrm{d}t\right\}\end{aligned} \tag{67}$$

where $s_i(t,\boldsymbol{\theta}) \triangleq s_{j(i),m_1(i),m_2(i)}(t;\boldsymbol{\theta})$ with $s_{j,m_1,m_2}(t;\boldsymbol{\theta})$ given in (5). Inserting (5) and (25) in (67) yields (24).

Appendix II
Technical Lemmas

Lemma 17 (Modified Version of [21, Observation 7.1.2]): Let $\beta \subset \{1, \ldots, n\}$ be an index set and $\mathbf{U}(\beta)$ and $\mathbf{V}(\beta)$ be the principal submatrices of the positive definite $n \times n$ matrices $\mathbf{U}$ and $\mathbf{V}$ formed by deleting the rows and columns complementary to those indexed by β. Then, we have

$$\mathbf{U} \succeq \mathbf{V} \Rightarrow \mathbf{U}(\beta) \succeq \mathbf{V}(\beta). \tag{68}$$

Proof: Let $\mathbf{x}$ be a vector with arbitrary entries in the components indicated by β and zero entries elsewhere. Let $\mathbf{x}(\beta)$ be the subvector of $\mathbf{x}$ indicated by β. Thus $\mathbf{x}^{\mathsf{H}}\mathbf{U}\mathbf{x} = \mathbf{x}(\beta)^{\mathsf{H}}\mathbf{U}(\beta)\mathbf{x}(\beta)$ and $\mathbf{x}^{\mathsf{H}}\mathbf{V}\mathbf{x} = \mathbf{x}(\beta)^{\mathsf{H}}\mathbf{V}(\beta)\mathbf{x}(\beta)$. The lemma follows from insertion into $\mathbf{x}^{\mathsf{H}}\mathbf{U}\mathbf{x} \geq \mathbf{x}^{\mathsf{H}}\mathbf{V}\mathbf{x}$. ∎

We remark that for positive definite matrices $\mathbf{Q}$ and $\mathbf{R}$

$$\mathbf{Q}^{-1} \succeq \mathbf{R}^{-1} \Leftrightarrow \mathbf{R} \succeq \mathbf{Q}. \tag{69}$$

A proof of (69) is given in [21, Th. 7.7.4].

Lemma 18: Let $\mathbf{Q}$ and $\mathbf{R}$ be $n \times n$ positive definite matrices and let $\beta \subset \{1, \ldots, n\}$ be an index set. Then the implication

$$\mathbf{R} \succeq \mathbf{Q} \Rightarrow [(\mathbf{Q}(\beta))^{-1}]_{p,p} \geq [(\mathbf{R}(\beta))^{-1}]_{p,p}, \quad p = 1, \ldots, n \tag{70}$$

holds.

Proof: From $\mathbf{R} \succeq \mathbf{Q}$ and Lemma 17, it follows that $\mathbf{R}(\beta) \succeq \mathbf{Q}(\beta)$. Then by (69), we have $(\mathbf{Q}(\beta))^{-1} \succeq (\mathbf{Q}(\beta))^{-1}$. Then Lemma 18 follows by applying Lemma 17. ∎

Lemma 19: A positive definite matrix $\mathbf{Q}$ fulfills $[\mathbf{Q}^{-1}]_{p,p} = 1/[\mathbf{Q}]_{p,p}$ for all p if and only if $\mathbf{Q}$ is diagonal.

Proof: It is easily checked that if $\mathbf{Q}$ is diagonal, then $[\mathbf{Q}^{-1}]_{p,p} = 1/[\mathbf{Q}^{-1}]_{p,p}$ for all p.

We now prove the converse, i.e., if $[\mathbf{Q}^{-1}]_{p,p} = 1/[\mathbf{Q}^{-1}]_{p,p}$ for all p, then $\mathbf{Q}$ is diagonal. Let $\mathbf{Q}_n = \mathbf{Q}$ be an $n \times n$ positive definite matrix and partition it as

$$\mathbf{Q}_n = \begin{bmatrix} \mathbf{Q}_{n-1} & \mathbf{j}_n \\ \mathbf{j}_n^{\mathsf{H}} & \eta_n \end{bmatrix} \tag{71}$$

where η is a scalar, $\mathbf{j}_n$ is a vector, and $\mathbf{Q}_{n-1}$ is the upper left $(n-1) \times (n-1)$ principal matrix of $\mathbf{Q}_n$. Inversion of $\mathbf{Q}_n$ yields

$$\left[\mathbf{Q}_n^{-1}\right]_{n,n} = \frac{1}{\eta_n + \mathbf{j}_n^{\mathsf{H}}\mathbf{Q}_{n-1}^{-1}\mathbf{j}_n}. \tag{72}$$

Assume that $[\mathbf{Q}_n^{-1}]_{p,p} = 1/[\mathbf{Q}_n]_{p,p}$ for all p and, therefore, in particular

$$\left[\mathbf{Q}_n^{-1}\right]_{n,n} = \frac{1}{[\mathbf{Q}_n]_{n,n}} = \frac{1}{\eta_n}. \tag{73}$$

Then (72) implies $\eta_n + \mathbf{j}_n^{\mathsf{H}}\mathbf{Q}_{n-1}^{-1}\mathbf{j}_n = \eta_n$ or $\mathbf{j}_n^{\mathsf{H}}\mathbf{Q}_{n-1}^{-1}\mathbf{j}_n = 0$. Since $\mathbf{Q}_n$ is positive definite, so is $\mathbf{Q}_{n-1}^{-1}$. Thus $\mathbf{j}_n^{\mathsf{H}}\mathbf{Q}_{n-1}^{-1}\mathbf{j}_n = 0$ if and only if $\mathbf{j}_n = \mathbf{0}$. To complete the proof, we repeat the argument for $\mathbf{Q}_{n-1}, \mathbf{Q}_{n-2}, \ldots, \mathbf{Q}_2$ to show that $\mathbf{j}_{n-1} = \mathbf{0}, \mathbf{j}_{n-2} = \mathbf{0}, \ldots, \mathbf{j}_2 = 0$ and thus $\mathbf{Q}_n$ is diagonal. ∎

Appendix III
Constant Volume Property of the Ambiguity Function

In the following, the ambiguity volume $V_{\mathrm{amb}} \triangleq \int_{\mathcal{E}} |\chi_0(\boldsymbol{\vartheta})|^2\,\mathrm{d}\boldsymbol{\vartheta}$ is derived. Making use of (49), some straightforward algebraic manipulations lead to (74) and (75) as shown at the top of the next page. The function $\mathrm{sinc}(\cdot)$ in (75) is defined as $\mathrm{sinc}(x) \triangleq (\sin(x)/x), x \neq 0$ and $\mathrm{sinc}(0) \triangleq 1$. We notice that the integral term $\int |p_i(t)|^2|p_{i'}(t)|^2\mathrm{d}t$ in (75) vanishes for index values i, i' such that $t(i) \neq t(i')$. Similarly, $\mathrm{sinc}(2\pi(d_k(i) - d_k(i')))$ is zero for i, i' such that $2(d_k(i) - d_k(i'))$ is an integer. Thus, by selecting spatiotemporal array such that for any i, i' with $t(i) = t(i')$, at least one of the quantities $2(d_1(i) - d_1(i'))$ and $2(d_2(i) - d_2(i'))$ is an integer, the terms $z_{i,i'}, i \neq i'$ are zero. This condition holds for

$$
\begin{aligned}
V_{\mathrm{amb}} &= \int_{\mathcal{E}} \left| \frac{1}{IE} \sum_{i=1}^{I} \int \exp(j2\pi(\nu t + d_1(i)\omega_1 + d_2(i)\omega_2)) |p_i(t)|^2 \mathrm{d}t \right|^2 \mathrm{d}\boldsymbol{\vartheta} \\
&= \frac{1}{(IE)^2} \int_{\mathcal{E}} \sum_{i=1}^{I} \int \exp(j2\pi(\nu t + d_1(i)\omega_1 + d_2(i)\omega_2)) |p_i(t)|^2 \mathrm{d}t \\
&\quad \times \sum_{i'=1}^{I} \int \exp\left(-j2\pi(\nu t' + d_1(i')\omega_1 + d_2(i')\omega_2)\right) |p_{i'}(t')|^2 \mathrm{d}t' \, \mathrm{d}\boldsymbol{\vartheta} = \frac{1}{(IE)^2} \sum_{i=1}^{I} \sum_{i'=1}^{I} z_{i,i'} \qquad (74) \\
z_{i,i'} &\triangleq \int \int |p_i(t)|^2 \, |p_{i'}(t')|^2 \int_{\mathcal{E}} \exp\left(j2\pi((t-t')\nu + (d_1(i) - d_1(i'))\omega_1 + (d_2(i) - d_2(i'))\,\omega_2)\right) \\
&\quad \times \mathrm{d}\boldsymbol{\vartheta} \, \mathrm{d}t \mathrm{d}t' \\
&= \int \int |p_i(t)|^2 |p_{i'}(t')|^2 \int_{-\infty}^{\infty} \exp(j2\pi(t-t')\nu) \mathrm{d}\nu \mathrm{d}t \mathrm{d}t' \\
&\quad \times \int_{-1}^{+1} \exp\left(j2\pi\left(d_1(i) - d_1(i')\right)\omega_1\right) \mathrm{d}\omega_1 \int_{-1}^{+1} \exp\left(j2\pi\left(d_2(i) - d_2(i')\right)\omega_2\right) \mathrm{d}\omega_2 \\
&= 4 \cdot \mathrm{sinc}\left(2\pi\left(d_1(i) - d_1(i')\right)\right) \cdot \mathrm{sinc}\left(2\pi\left(d_2(i) - d_2(i')\right)\right) \cdot \int |p_i(t)|^2 |p_{i'}(t)|^2 \mathrm{d}t \qquad (75)
\end{aligned}
$$

switched sounding systems where $i \neq i' \Leftrightarrow t(i) \neq t(i')$. The condition also holds for systems equipped with uniform linear arrays with half-wavelength interelement spacing.

For a spatiotemporal array such that $z_{i,i'} = 0$, $i \neq i'$ the ambiguity volume reads

$$
V_{\mathrm{amb}} = \frac{4 \sum_{i=1}^{I} z_{i,i}}{(IE)^2} = \frac{4 \sum_{i=1}^{I} \int |p_i(t)|^4 \mathrm{d}t}{(IE)^2}. \qquad (76)
$$

Thus, for this class of spatiotemporal arrays, the ambiguity volume depends only on the second-order moment E and fourth-order moments $\int |p_i(t)|^4 \mathrm{d}t$, $i = 1, \ldots, I$, of the transmitted sounding pulses.

ACKNOWLEDGMENT

The authors would like to thank Prof. A. Renaux and Prof. P. Larzabal for their generous and helpful comments and suggestions.

REFERENCES

[1] S. Salous, P. Filippidis, R. Lewenz, I. Hawkins, N. Razavi-Ghods, and M. Abdallah, "Parallel receiver channel sounder for spatial and MIMO characterisation of the mobile radio channel," *Proc. Inst. Electr. Eng. —Commun.*, vol. 152, no. 6, pp. 912–918, Dec. 2005.

[2] B. H. Fleury, M. Tschudin, R. Heddergott, D. Dahlhaus, and K. L. Pedersen, "Channel parameter estimation in mobile radio environments using the SAGE algorithm," *IEEE J. Sel. Areas Commun.*, vol. 17, pp. 434–450, Mar. 1999.

[3] B. H. Fleury, P. Jourdan, and A. Stucki, "High-resolution channel parameter estimation for MIMO applications using the SAGE algorithm," in *Proc. Int. Zurich Seminar Broadband Commun.*, Feb. 2002, vol. 30, pp. 1–9.

[4] X. Yin, B. Fleury, P. Jourdan, and A. Stucki, "Doppler frequency estimation for channel sounding using switched multiple-element transmit and receive antennas," in *Proc. IEEE Global Telecommun. Conf. (IEEE GLOBECOM)*, Dec. 2003, vol. 4, pp. 2177–2181.

[5] T. Pedersen, C. Pedersen, X. Yin, B. H. Fleury, R. R. Pedersen, B. B. A. Hviid, P. Jourdan, and A. Stucki, "Joint estimation of Doppler frequency and directions in channel sounding using switched TX and RX arrays," in *Proc. IEEE Global Telecommun. Conf. (IEEE GLOBECOM)*, Dec. 2004, vol. 4, pp. 2354–2360.

[6] A. N. Mirkin and L. H. Sibul, "Cramér-Rao bounds on angle estimation with a two-dimensional array," *IEEE Trans. Signal Process.*, vol. 39, pp. 515–517, Feb. 1991.

[7] R. O. Nielsen, "Azimuth and elevation angle estimation with a three-dimensional array," *IEEE J. Ocean. Eng.*, vol. 19, pp. 84–86, Jan. 1994.

[8] P. M. Woodward, *Probability and Information Theory, With Applications to Radar*, 2nd ed. New York: Pergamon, 1964.

[9] M. J. D. Rendas and J. M. F. Moura, "Ambiguity in radar and sonar," *IEEE Trans. Signal Process.*, vol. 46, pp. 294–305, Feb. 1998.

[10] H. L. V. Trees, *Detection, Estimation, and Modulation Theory*. New York: Wiley, 1971, Radar-Sonar Signal Processing and Gaussian Signals in Noise, pt. 3.

[11] G. S. Antonio, D. R. Fuhrmann, and F. C. Robey, "MIMO radar ambiguity functions," *IEEE J. Sel. Topics Signal Process.*, vol. 1, pp. 167–177, Jun. 2007.

[12] P. J. Cullen, P. C. Fannin, and A. Molina, "Wide-band measurement and analysis techniques for the mobile radio channel," *IEEE Trans. Veh. Technol.*, vol. 42, pp. 589–603, Nov. 1993.

[13] P. C. Fannin and A. Molina, "Analysis of mobile radio channel sounding measurements in inner Dublin at 1.808 GHz," *Proc. Inst. Electr. Eng.—Commun.*, vol. 143, no. 5, pp. 311–316, Oct. 1996.

[14] L. C. Godara and A. Cantoni, "Uniqueness and linear independence of steering vectors in array space," *J. Acoust. Soc. Amer.*, vol. 70, no. 2, pp. 467–475, Aug. 1981.

[15] J. T.-H. Lo, J. Stanley, and L. Marple, "Observability conditions for multiple signal direction finding and array sensor localization," *IEEE Trans. Signal Process.*, vol. 40, pp. 2641–2650, Nov. 1992.

[16] K.-C. Tan, S. S. Goh, and E.-C. Tan, "A study of the rank-ambiguity issues in direction-of-arrival estimation," *IEEE Trans. Signal Process.*, vol. 44, pp. 880–887, Apr. 1996.

[17] H. V. Poor, *An Introduction to Signal Detection and Estimation*. New York: Springer-Verlag, 1988.

[18] H. L. V. Trees, *Detection, Estimation, and Modulation Theory*. New York: Wiley, 1968, Detection, Estimation and Linear Modulation Theory, pt. 1.

[19] W. J. Bangs, "Array Processing With Generalized Beam-Formers," Ph.D. dissertation, Yale Univ., New Haven, CT, 1971.

[20] L. L. Scharf, *Statistical Signal Processing: Detection, Estimation, and Time Series Analysis*. Reading, MA: Addison-Wesley, 1991.

[21] R. A. Horn and C. A. Johnson, *Matrix Analysis*. Cambridge, U.K.: Cambridge Univ. Press, 1985.

[22] A. Dogandžić and A. Nehorai, "Space-time fading channel estimation and symbol detection in unknown spatially correlated noise," Dept. Elect. Eng. Comput. Sci., Univ. Illinois, Chicago, Tech. Rep. UIC-EECS-00-9, 2000.

[23] A. Dogandžić and A. Nehorai, "Space-time fading channel estimation and symbol detection in unknown spatially correlated noise," *IEEE Trans. Signal Process.*, vol. 50, pp. 457–474, Mar. 2002.

[24] C. Balanis, *Antenna Theory: Analysis and Design*, 2nd ed. New York: Wiley, 1997.
[25] R. J. McAulay and E. M. Hofstetter, "Barankin bounds on parameter estimation," *IEEE Trans. Inf. Theory*, vol. IT-17, pp. 669–676, Nov. 1971.
[26] D. C. Rife and R. R. Boorstyn, "Single tone parameter estimation from discrete-time observations," *IEEE Trans. Inf. Theory*, vol. IT-20, pp. 591–598, Sep. 1974.
[27] S. D. Howard and P. Lavoie, "Analysis of SNR threshold for differential Doppler frequency measurement in digital receivers," in *Proc. 2000 IEEE Int. Conf. Acoust., Speech, Signal Process. (ICASSP)*, Jun. 2000, vol. 1, pp. 289–292.
[28] F. Athley, "Performance analysis of DOA estimation in the threshold region," in *Proc. IEEE Int. Conf. Acoust., Speech, Signal Process. (ICASSP)*, May 2002, vol. 3, pp. 3017–3020.
[29] F. Athley, "Threshold region performance of maximum likelihood direction of arrival estimators," *IEEE Trans. Signal Process.*, vol. 53, pp. 1359–1373, Apr. 2005.
[30] S. S. Haykin, *Adaptive Filter Theory*. Englewood Cliffs, NJ: Prentice-Hall, 2002.

Troels Pedersen (S'04) received the M.Sc.E. degree in digital communications from Aalborg University, Denmark, in 2004, where he is currently pursuing the Ph.D. degree in wireless communications.

His research interests lie in the area of statistical signal processing and communication theory, including sensor array signal processing, wireless localization techniques, radio channel modelling, and radio channel sounding.

Claus Pedersen received the M.Sc.E. degree in digital communications from Aalborg University, Denmark, in 2004.

He is currently a DSP Developer with a company in the Danish telecommunications industry. His engineering interests lie in a broad range of areas within digital communications. Among these are modulation techniques, error control coding, and adaptive and interactive algorithms for filtering, equalization, and estimation.

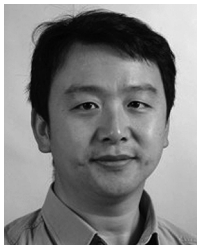

Xuefeng Yin (S'02–M'06) was born in Hebei, China, 1973. He received the B.S. degree in optoelectronics from Huazhong University of Science and Technology, China, in 1995 and the M.Sc.E. degree in digital communications and the Ph.D. degree in wireless communications from Aalborg University, Denmark, in 2002 and 2006, respectively.

From 1995 to 2000, he was a System Engineer with Motorola Cellular Infrastructure Corporation, Hangzhou, China. Since August 2006, he has been an Assistant Professor in the Section Navigation and Communications, Department of Electronic Systems, Aalborg University. His research interests are in sensor array signal processing, parameter estimation for radio channel, channel characterization, target tracking, and identification in radar applications.

Bernard H. Fleury (M'97–SM'99) received the Diploma degree in electrical engineering and mathematics in 1978 and 1990, respectively, and the Ph.D. degree in electrical engineering from the Swiss Federal Institute of Technology Zurich (ETHZ), Switzerland, in 1990.

From 1978 to 1985 and 1988 to 1992, he was, respectively, a Teaching Assistant and a Research Assistant at the Communication Technology Laboratory and at the Statistical Seminar at ETHZ. In 1992, he rejoined the former laboratory as a Senior Research Associate. Since 1997, he has been with the Department of Electronic Systems, Aalborg University, Denmark, as a Professor in communication theory. He is the Head of the Section Navigation and Communications, one of the eight laboratories of this department. Since April 2006, he has also been a Key Researcher with ftw. Forschungszentrum Telekommunikation Wien, Austria, where he is Manager of the Research Area Signal and Information Processing. His general fields of interest cover numerous aspects within communication theory and signal processing, mainly for wireless communications. His current areas of research include stochastic modelling and estimation of the radio channel, especially for multiple-input multiple-output applications and in fast time-varying environments, and iterative information processing with focus on efficient, feasible advanced receiver architectures. He has authored and coauthored more than 90 publications in these areas. He has developed with his staff a high-resolution method for the estimation of radio channel parameters that has found a wide application and has inspired similar estimation techniques both in academia and in industry.